INVESTIGATION OF PHOTOCATALYTIC EFFECT OF WO_3/SnO_2 THIN FILMS FOR CONTAMINATED WATER TREATMENT

VICTOR ISAHI

A Thesis Submitted to the Institute of Postgraduate Studies of Kabarak University in Partial Fulfillment of the Requirements for the Award of Master of Science in Physics

KABARAK UNIVERSITY

NOVEMBER, 2023

DECLARATION

1. I do declare that:
    i. This thesis is my original work and to the best of my knowledge, it has not been presented to any institution as a research paper for the award or conferment of any academic degree or diploma.
    ii. That the work has not incorporated material from other works or a paraphrase of such material without due and appropriate acknowledgement.
    iii. That the work has been subjected to the process of anti-plagiarism and has met Kabarak University 15% similarity index threshold.
2. I do understand that issues of academic integrity are paramount and therefore I may be suspended or expelled from the university or my degree be recalled for academic honesty and other related malpractices.

Signature:**.....** Date:.....

Victor Isahi

GMP/M/1895/09/20

RECOMMENDATION

To the institute of Postgraduate Studies:

The research thesis titled **"Investigation of Photocatalytic effect of WO_3/SnO_2 Thin Films for Contaminated Water Treatment"** and written by **Victor Isahi** is presented to the Institute of Postgraduate Studies of Kabarak University. We have reviewed the thesis and recommend it be accepted in partial fulfillment of the requirement for award of the Master of Science in Physics.

Signature:..... Date:.....

Prof. Christopher Maghanga

Professor of Physics, Department of Biological & Physical Sciences

Kabarak University

Signature:..... Date:.....

Prof. Maurice M. Mwamburi

Professor of Physics, Department of Physics

University of Eldoret, Kenya

Signature:..... Date:.....

Dr. Onesmus Munyati

Senior Lecturer, Department of Chemistry

University of Zambia

ACKNOWLEDGMENTS

I would like to sincerely thank God for his grace throughout this study. My sincere gratitude to my research supervisors Professor Christopher Maghanga, Professor Maurice Mwamburi, and Dr. Onesmus Munyati for their positive and timely guidance. I also appreciate both the teaching and non-teaching staff of Kabarak University and the University of Zambia for their involvement in my research. I am also thankful to Prof. Reccab Manyala and Dr. Sylvester Hatwaambo for their inspiration and support throughout my stay in Zambia. Further, I would like to thank my colleagues Emmanuel Akoto and Wycliffe Isoe for their support during this study. Lastly, I acknowledge the International Science Programme (ISP) of Uppsala Sweden, and the Materials Science &Solar Energy Network for Eastern and Southern Africa (MSSEESA) for supporting and funding this work.

DEDICATION

I dedicate this thesis to my parents Judith and Evans Mutange, siblings: Lynn Bora, Grace Mbambale and Emmanuel Akoto for their never-ending love, encouragement, and support.

ABSTRACT

Removal of pollutants in water has been a challenge and poses significant risk to human health. As a result, research initiatives aimed to eliminate these pollutants have been on the rise. Photocatalysis has shown incredible potential for water treatment since it is affordable and utilizes solar energy. Tin (IV) Oxide (SnO_2) has ardently been investigated as a photocatalyst for water treatment due to its remarkable properties, non-toxicity, and stability. However, its wide-bandgap and the tendency for some electrons and holes to recombine have been cited among the limiting factors. This study, therefore, aimed at preparing and optimizing Tin (IV) Oxide (SnO_2) thin film by doping it with varied proportions of Tungsten (VI) Oxide (WO_3) and to investigate the effect of WO_3 doping on the optical, structural and photocatalytic properties of the prepared samples. PureSnO_2 and five groups of WO_3/SnO_2 (WO_3 of 0.1, 0.3, 0.5, 1.5, and 2.0 wt.%) thin films were successfully fabricated through Sol-gel Spin coating technique at a rotary speed of 1200rpm for 30 seconds followed by annealing at 500 ºC for 1hr. The average thickness of the prepared films was 135.4 nm. The photocatalytic properties of the prepared samples were analyzed by studying the photo degradation of methylene blue dye under UV light. The calculated rate constants for undoped SnO_2 was 0.00256 min^{-1} while WO_3/SnO_2 (1.5%wt.) yielded a degradation rate constant of 0.00519 min^{-1} which was twice that of pure SnO_2 films. The mechanism involved in the enhancement of the photocatalytic efficiency of the SnO_2 thin film due to the addition of WO_3 is explained based on optical and structural characterization. Doping improved the optical absorbance of the films and caused a red shift on the absorption edge of the films, decreasing the band gap from 3.82 to 3.03 eV. X-ray Diffraction (XRD) studies revealed that the prepared samples were, polycrystalline in structure, with the crystallite size of pure SnO_2 increasing after being doped byWO_3. These results show that low-cost WO_3/SnO_2 photocatalyst is a good candidate to eliminate organic pollutants from contaminated water, which cause severe threats to health and the environment.

Keywords: *Photocatalysis, Tin (IV) Oxide, Tungsten (VI) Oxide, Pollutants*

TABLE OF CONTENTS

LIST OF TABLES

LIST OF FIGURES

LIST OF SYMBOLS, ACRONYMS, AND ABBREVIATION

$\alpha(\lambda)$	Absorption Coefficient as a Function of Wavelength
A(λ)	Absorbance as a function of wavelength
AFM	Atomic-Force Microscopy
Ag	Silver
BET	Brunauera–Emmett–Teller
c	Speed of Light
CB	Conduction Band
DRS	Diffuse Reflectance Spectroscopy
Eg	Energy Band Gap
EHP	Electron-hole Pair
EDS	Energy Dispersive Spectroscopy
Ev	Electron Volts
FTIR	Fourier Transform Infrared
FESEM	Field Emission Scanning Electron Microscopy
FWHM	Full Width Half Maximum
GO	Graphene Oxide
h	Planck's constant
HTREM	High-resolution transmission electron microscopy
I_0	Total Intensity of Incident Radiation
I_A	Amount of light absorbed
I_R	Amount of light reflected
I_T	Amount of light transmitted
k_c	Kinetic rate constant
$k(\lambda)$	Extinction coefficient
n	Refractive Index
NACOSTI	National Commission for Science, Technology and Innovation
NPs	Nanoparticles
NSs	Nano-Sheets
PL	Photoluminescence
R(λ)	Reflectance as function of wavelength
SnO_2	Tin (IV) Oxide

$SnCl_2 \cdot 2H_2O$	Tin (II) Chloride Dihydrate
SEM	Scanning Electron Microscopy
SDGs	Sustainable Development Goals
SILAR	Successive Ionic Layer Adsorption and Reaction
$T(\lambda)$	Transmittance as a Function of Wavelength
TEM	Transmission Electron Microscopy.
TiO_2	Titanium Dioxide
UV/VIS-NIR	Ultraviolet-Visible Near-Infrared
UV	Ultraviolet
VB	Valence Band
WO_3	Tungsten (VI) Oxide
WHO	World Health Organization
W	Tungsten
WCl_6	Tungsten hexachloride
XPS	X-ray photoelectron spectroscopy
XRD	X-Ray Diffraction
ZnO	Zinc Oxide

OPERATIONAL DEFINITION OF TERMS

Photocatalysis: It is the acceleration of a photoreaction in the presence of a photocatalyst.

Sol-gel method: It is a wet-chemical technique for the synthesis of nanostructures such as thin films and nanoparticles, especially metal oxides.

Tin (IV) oxide: This is a semiconductor with a chemical formula SnO_2 and a wide direct band gap of about 3.7eV to 4.2eV.

Doping: It is the introduction of an impurity into an intrinsic (pure) semiconductor to modify its properties.

Morphology: Is the study of the shapes, sizes, and structures of nanostructured materials.

Optical Properties: It is the interaction of a material with light which includes its absorbance, transmittance, and reflectance.

CHAPTER ONE

INTRODUCTION

1.1 Introduction

This chapter entails the problem that motivated this study, the objectives, and the research questions which guided this research. In addition, the justification, scope of the study, limitations, and assumptions made are also discussed.

1.2 Background to the Study

Photocatalysis is the acceleration of a photoreaction in the presence of a semi-conductor photocatalyst (McNaught, 1997). It forms one of the alternatives for contaminated water treatment (Hariganesh *et al.*, 2020). It is based on the reaction between organic contaminants in water and powerful oxidizing and reducing agents (h^+ and e^-) generated by the Ultraviolet (UV) or visible light on the photocatalysts surface(Hasija *et al.*, 2019). In contrast to other methods, it possesses advantages because of simplicity, low cost, non-toxicity, eco-friendliness, complete degradation of pollutants, as well as the possibility of utilizing solar light(Ali *et al.*, 2017; Zhu & Zhou, 2019).

At the moment, metal oxide photocatalysts such as Titanium dioxide (TiO_2), Zinc Oxide (ZnO), and Tin (IV) Oxide (SnO_2) have shown promising performance in the elimination of organic pollutants (Chatterjee & Dasgupta, 2005; Han *et al.*, 2014; Iqbal *et al.*, 2018; Manikandan et al., 2018)however, they have low efficiency because of wide-bandgap and high electron-hole pair recombination(Ishchenko *et al.*, 2021). This hinders Tin (IV) Oxide (SnO_2) from being widely and practically used in pollution degradation.

According to Koohestani, (2019), enhancement in photocatalytic performance is due to improvement in optical properties i.e. light absorption properties, and reduction in the

recombination rate of the electron-hole pairs produced by light.Studies suggest that doping significantly improves the optical and photocatalytic properties of SnO_2 (Table 1). As a result, endeavors to create useful photocatalysts through doping are on the rise.

Dopants, such as Ag^+, WO_3, and W have previously been reported to improve the photocatalytic execution properties of oxide catalysts particularlyTiO_2(Behnajady et al., 2006; Ramos-Delgado et *al.,* 2013; Y. Wang *et al.,* 2016). In the presence of radiation, the dopants act as electron-accepting species, thereby improving the photocatalytic activity(Y. Wang *et al.,* 2016). It follows therefore that WO_3 as a dopant can serve to decrease the recombination rate of SnO_2 photocatalyst hence improving its photocatalytic properties. Despite extensive studies that have been done on WO_3 andSnO_2, there is limited information on the combined use of these two materials through doping for photocatalytic water treatment applications. Some of the works based on doping $SnO_2$are presented in Table 1.

Table 1

Summary of some Selected Works on Doped SnO_2 thin films for Photocatalytic Studies.

Reference	Title of Study	Key findings
(Manikandan *et al.*, 2018)	Ag activated SnO_2 films for enhanced photocatalytic dye degradation against toxic organic dyes	Doping decreased the bang gap of pureSnO_2 from 3.5eV and 3.2 eV. $SnO_2:Ag$ film has better photocatalytic activity thanSnO_2
(Raj *et al.*, 2020)	Study on the synergistic effect of terbium-doped SnO_2 thin-film photocatalysts for dye degradation	Tb doping with SnO_2increased absorbance, and decreased the bandgap values providing more photon absorption which enhanced the photocatalytic reaction improving the rate constant
(Zarei *et al.*, 2022)	Photocatalytic properties of ZnO/SnO_2 nanocomposite films: role of morphology	The ZnO/SnO_2film had a higher photodegradation rate of MB dye under ultraviolet irradiation, than pristine ZnO and SnO_2films due to effective separation of hole–electron pairs
(Azim *et al.*, 2021)	$GO-SnO_2$Nanocomposite for Photodegradation of Methyl Orange Under Direct Sunlight Irradiation and Mechanism	The Wide bandgap of SnO_2 was tuned using GO which showed enhanced photocatalytic performance with greater surface area compared to pure SnO_2
(Doyan *et al.*, 2019)	The Effect of Indium Doped SnO_2 Thin Films on Optical Properties Prepared by Sol-Gel Spin Coating Technique	SnO_2Thin films underwent a drop in bandgap from 3.64 to 3.57 eV with increase in doping.

In this research, the choice of Tungsten (VI) Oxide (WO_3) and Tin (IV) Oxide (SnO_2) is because of their remarkable optical and structural properties, non-toxicity, thermal stability, chemical stability, good photostability and low-cost metal precursors (Ishchenko *et al.*, 2021; Nandiyanto *et al.*, 2013; P. Singh et al., 2019; Y. Wang *et al.*, 2016).

The WO_3/SnO_2thin film synthesis can be done using a variety of techniques including Sol-gel, Spray pyrolysis, Electroless deposition, Electroplating, Chemical bath deposition, Chemical vapor deposition, Evaporation, and Sputtering(Jilani *et al.*, 2017). Among the methods, Sol-gel is a simple, fast, and low cost technique. It has several advantages such as controlled stoichiometry, better homogeneity, low processing temperature, high purity, effective control of properties such as film thickness, and the ability to easily scale up (Chaudhary, 2021; Huang et al., 2021; Parashar *et al.*, 2020; Tseng *et al.*, 2010).

Keeping the aforementioned in mind in this study, controlled coupling by varying the proportion ofWO_3 in SnO_2wasdone using the Sol-gel spin coating technique, and the optical, structural, and photocatalytic properties of the prepared samples investigated though spectrometric studies, X-Ray diffraction studies and by methylene blue (MB) dye degradation studies under UV lightrespectively. Tin (IV) Oxide (SnO_2) was optimized for photocatalytic water treatment activity.

1.3 Statement of the Research Problem

Globally 1 in 3 individuals living today do not have adequate access to clean and safe drinking water(United Nation, 2022). A World Health Organization (WHO) report indicated that contaminated drinking water can spread illnesses such as; diarrhea, cholera, dysentery, typhoid, and polio and are projected to cause many deaths annually(Buchholz, 2022; World Heath Organization, 2022). Organic substances form one of the major pollutants in contaminated water(G. Singh et al., 2021), as a result of effluents containing toxic dyes discharged from various industries that contaminate rivers and other water resources (Manikandan et al., 2018; Ojha & Tiwary, 2021). Therefore, research related to finding affordable, effective, and healthy approaches to

eliminate these toxic dyes has been on the rise in recent years. Most procedures designed to remove these pollutants are via flocculation, coagulation, precipitation, biological oxidation, ion exchange, adsorption, and membrane processing (Piaskowski et al., 2018; J. Sun et al., 2015). These techniques are often inefficient, slow, costly, and unfeasible for large-scale applications or have other limitations (Crini & Lichtfouse, 2019). Hence there is a need to utilize an affordable, effective and healthy approach. Photocatalysis has shown incredible potential because of its advantages(Katwal et al., 2021). Tin (IV) Oxide (SnO_2) Photocatalyst has been investigated for water treatment but electron-hole pair recombination, wide bandgap, and poor light absorption have been stated among the limiting factors(Azim et al., 2021). Research shows that doping expands the light absorption range, promotes the generation of charge carriers, and improves electron-hole separation(M. Sun et al., 2019), increasing the likelihood of charge carriers taking part in photocatalysis. While doping is regarded as the most effective method for increasing absorption capacity, exceeding a particular limit reduces absorption, lowering the material's photocatalytic activity (Chebwogen et al., 2019).Hence there is need to find the optimum dopant proportion for an efficient photocatalyst. In this work, the influence of Tungsten (VI) Oxide (WO_3) doping on Tin (IV) Oxide (SnO_2) was studied to ascertain the best preparation and characterization parameters that would produce an efficient WO_3/SnO_2 photocatalyst.

1.4 Objectives of the Study

1.4.1 Main Objective of the Study

The primary objective of this study was to investigate the photocatalytic influence of WO_3 doping on SnO_2 for contaminated water treatment.

1.4.2 Specific Objectives of the Study

The specific objectives in this research were:

i. To prepare thin films by the Sol-gel method with varying proportions of WO_3 in SnO_2.

ii. To investigate optical properties of the prepared WO_3/SnO_2 photocatalyst thin films.

iii. To investigate structural properties of the prepared WO_3/SnO_2.

iv. To test the photocatalytic activity of SnO_2 and WO_3/SnO_2 thin films by subjecting them to the methylene blue dye degradation test.

1.5 Research Questions

i. What is the optimal dopant proportion of WO_3 in WO_3/SnO_2 for an efficient photocatalyst thin film?

ii. What are the optical properties of the prepared WO_3/SnO_2 photocatalyst thin films?

iii. What are the structural properties of the prepared WO_3/SnO_2?

iv. What is the difference in photocatalytic activity of the pure SnO_2 and optimized WO_3/SnO_2 thin films?

1.6 Justification of the Study

Water contamination is a pressing global issue because of the increased number of deaths caused by water-borne diseases (Buchholz, 2022; World Heath Organization, 2022). This necessitates finding environment-friendly and low-cost approaches that do not need well-developed infrastructure to treat water. Photocatalysis has shown incredible potential since it is affordable, effective and eco-friendly. However, the low efficiency of commonly used photocatalysts such as Tin (IV) Oxide (SnO_2) has been a limiting factor.

To address this problem, it is feasible to increase efficiency by modifying the optical &structural properties of Tin (IV) Oxide (SnO_2) thin films through doping it with a suitable dopant such as Tungsten (VI) Oxide (WO_3) through the sol-gel synthesis, which is an effective technique to create excellent metal oxide nanostructures as opposed to other methods. Additionally. Thin films are highly attractive because they can be coated large areas suitable for industrial applications.

The findings of this research contributes to improving the photocatalytic efficiency of Tin (IV) Oxide (SnO_2), therefore moving a step closer to a broad use of photocatalytic water treatment, which is an effective, affordable and healthy approach. Hence contributing in enhancing the Kenya Vision 2030 'which aims to transform Kenya into a newly industrializing, middle-income country providing a high-quality life to all its citizens by 2030 in a clean and secure environment' and the Sustainable Development Goals; SDG 6 (Clean water and sanitation) and SDG 3 (Good health and well-being).

1.7 Scope of the Study

This research focused on the Optical & structural properties of Tin (IV) Oxide (SnO_2) doped with Tungsten (VI) Oxide (WO_3) prepared by the sol-gel method and its Photocatalytic activity. Therefore the findings of this study may not be generalized to Tin (IV) Oxide doped with Tungsten (VI) Oxide prepared by other methods.

1.8 Limitation of the Study

The main limitation of this study is that the available X-Ray Diffraction (XRD) equipment for structural characterization was a powder XRD, which could not be used to characterize the thin films. However to investigate the influence of doping on crystal structure, nanoparticles were prepared.

1.9 Assumption of the Study

This study assumed that the properties of the prepared Tin (IV) Oxide doped with Tungsten (VI) Oxide (WO_3/SnO_2) were not influenced by changes in physical conditions such as humidity and temperature. This is assumed because Tin (IV) oxide is known to be stable.

CHAPTER TWO

LITERATURE REVIEW

2.1 Introduction

This section reviews the historical backdrop of photocatalysis, it presents related work done by different scientists in connection to the preparation and properties of SnO_2 and WO_3/SnO_2. In addition, it explains the theory of photocatalytic thin films, their optical, morphological, and structural properties, and their applications in water treatment. The conceptual framework and a summary of the research gaps are also presented.

2.2 Empirical review of Work done on Photocatalysis,SnO_2, and WO_3/SnO_2.

2.2.1 Photocatalysis

In the late 1960s and early 70s, Fujishima andHonda found a relatively inexpensive and widely available material, titanium dioxide, that acts as a photocatalyst when it is exposed to UV light (Britannica, 2022). The findings of Fujishima &Honda led to other advances in photocatalysis.To date, several photocatalyst compounds have been investigated. Titanium (IV) Oxide (TiO_2) has been the most thoroughly studied photocatalyst material because it possesses a lot of advantages (Moma & Baloyi, 2019). Tin (IV) Oxide (SnO_2) has likewise been ardently explored for water purification and environment decontamination(Azim et al., 2021). All this is aimed at improving the efficiency of this material for the broad application of photocatalysis.

Since the discovery by Fujishima and Honda several materials have been studied for their potential in photocatalysis and properties which makes them useful for application in photocatalysis. Several important parameters have been studied and reported to be taken into consideration when producing excellent photocatalyst materials. This parameters include;

i. The type of material (Badli et al., 2017; Nadarajan et al., 2018; Radhika et al., 2019; Sakthivel et al., 2003; Vamvasakis et al., 2015)

ii. Photocatalyst size, morphology, and surface chemistry(Arutanti et al., 2014; Nagaveni et al., 2004; Nandiyanto et al., 2009, 2013)

iii. Crystallite size and structure(Cheng et al., 2010)

iv. Additional co-catalyst and doped material (Abdullah et al., 2016; Alshammari et al., 2019; Arai et al., 2008; Armaković et al., 2019; Arutanti et al., 2014; Badli et al., 2017; Nadarajan et al., 2018)

v. Photocatalytic process condition (e.g. pH, temperature, illumination time, radiation intensity) (Nandiyanto et al., 2016; Sakthivel et al., 2003; Zhang et al., 2007)

vi. Stoichiometrical composition between reactant and catalyst in the photodecomposition process (Churbanov et al., 2007; Hayashi et al., 2003; Sakthivel et al., 2003; Szilagyi et al., 2008)

2.2.2. Tin (IV) Oxide (SnO_2)

A review done by Al-Hamdi et al., 2017on Tin (IV) Oxide as a photocatalyst for water treatment showed that despite Tin (IV) Oxide semiconductor having significant potential for photocatalytic applications, the applicability of the pure $SnO_2$is limited because of the high activation energy of the compound and swift recombination rate of the photogenerated electrons and holes. He concluded that to enhance the photocatalytic activity, the Electron-Hole-Pair recombination needs to be addressed through doping the material. Due to this, a need was created to find a suitable dopant material to avert these issues.

Haouanoh et al., 2019deposited Tin (IV) oxide (SnO_2) thin films by the Sol-gel dip-coating technique on glass substrates. He studied the influence heat treatment and number of layers on structural, morphological, optical, and electrical properties. The XRD Spectra revealed that the preheated temperature, number of layers, and annealing temperature strongly influence the size of crystallites. UV-Vis spectroscopy showed significant transparency in the infrared and visible domains (75%–96%). For all films, the energy band gap was found to vary randomly with the preheated temperature; it increased from 3.83 eV - 3.88 eV for three-layer and six-layer films respectively. This shows that the preparation parameters are important to obtain a material of suitable structural& optical properties for photocatalytic water treatment.

Patel et al., 2021synthesized Tin (IV) Oxide (SnO_2) by sol-gel method. Using X-ray Diffraction, Scanning Electron Microscopy, and Transmission Electron Microscopy for characterization, he found out that the synthesized nanoparticles had a SnO_2 phase with a tetragonal unit cell crystal structure with a direct band gap of 3.64 eV, and were well-oriented, spherical in shape and polycrystalline. This showed that SnO_2 is a promising photocatalytic material.

Yıldırım et al., 2012used the Successive Ionic Layer Adsorption and Reaction (SILAR) method to deposit Tin (IV) Oxide (SnO_2) thin films on glass substrates at room temperature. The influence of film thickness on structural, optical, morphological, & electrical properties of the films was investigated. In addition, the films were annealed in an oxygen atmosphere for 30 minutes at 400°C, and the film's characteristic parameters were investigated. X-ray Diffraction (XRD) and Scanning Electron Microscopy (SEM) analyses revealed that all of the films were polycrystalline with a tetragonal structure and were well covered on glass substrates. An examination of the crystalline and surface properties of the films, showed improvement with increasing film thickness. As the film

thickness increased from 215 to 490 nm, the optical band gap decreased from 3.90 eV to 3.54 eV and the electrical conductivity changed from 0.015 to 0.815 $(\Omega\text{-cm})^{-1}$. The optical band gap values as a function of film thickness were used to calculate the refractive index (n). It was discovered that the thin films that were dense, uniform, smooth, and well-adhered to the substrates. Also, the level of surface roughness increased as the film surface deteriorated. When compared to the as-deposited film, the annealed film surface was better, more compact, denser, and more uniform. By annealing, the grains combined to form a crystalline film, hence increasing grain size. As a result, the surface properties of Tin (IV) Oxide thin films were concluded to vary significantly with film thickness and annealing temperature.

The decrease in band gap with increasing film thickness was attributed to crystallinity improvement, morphological changes, atomic distance changes, and grain size changes. During the growth process, it was discovered that some impurity levels (oxygen vacancies and/or Sn interstitials, for example) increase near the conduction band as film thickness increases. Furthermore, structural defects in the films were discovered to be due to their preparation conditions, which could have given rise to the allowed states near the conduction band in the forbidden region. With increasing film thickness, these allowed states may have merged with the conduction band, resulting in a reduction of the band gap. They also noted that the decrease in band gap with annealing temperature was due to improved crystallinity &surface properties, in addition to the elimination of tin hydroxide formation along grain boundaries, which is a more common phenomenon in chemically deposited thin films. These findings show that preparation parameters such as annealing temperature and film thickness have a significant impact on the properties of prepared Tin (IV) Oxide thin film.

Marikkannan et al. 2015 synthesized Tin oxide thin films for optoelectronic applications using the sol-gel spin coating process on glass substrates at room temperature using three different solvents: isopropanol, ethanol, and methanol. X-ray diffraction (XRD), Fourier transform infrared (FTIR) spectroscopy, atomic force microscopy (AFM), UV-vis spectroscopy, photoluminescence (PL) analysis, and Raman spectroscopy were used to characterize the variations in the structural, optical, and morphological properties of thin films deposited with different solvents. The XRD patterns indicated that all of the films were polycrystalline in nature and contained a mixed phase of tin (IV) oxide and tin (II) oxide in a metastable orthorhombic crystal structure, regardless of the solvents used for preparation. The presence of Sn=O and Sn-O was confirmed by FTIR spectra in all of the samples. For all solvents, PL spectra revealed a violet emission band centered at 380 nm (3.25 eV). The UV-vis spectra revealed a maximum absorption band at 332 nm and a high average transmittance of around 97% for thin film samples synthesized with isopropanol and methanol. The AFM results show that the grain size varies with solvent.

The grain sizes of tin Oxide prepared with Isopropanol, Ethanol, and Methanol were measured to be 62, 74, and 94 nm, respectively. Showing that thin films prepared by methanol gives the highest grain size. Grain size significantly influences the properties of a photocatalyst thin film. The optical & structural properties of the prepared thin films suggested that this method of fabricating tin oxide is promising, and that additional work is needed to analyze the electrical properties of the films to determine their viability for various transparent conducting oxide applications. This work clearly demonstrates that the solvent utilized prepare Tin (IV) Oxide thin films has a substantial effect on a number of their properties, which are also very critical for photocatalytic applications.

2.2.3. Doped Tin (IV) Oxide (SnO_2) Photocatalyst

Azim et al., 2021 modified Tin (IV) Oxide (SnO_2) properties by doping it with Graphene Oxide (GO) for Photodegradation of Methyl Orange under direct sunlight irradiation. He found out that; Modifying Tin (IV) Oxide (SnO_2) by doping can narrow its wide bandgap and enhance the photogenerated charge separation, the synthesized Graphene Doped-Tin Oxide nanoparticles showed an efficient photodegradation of 94% for Methyl Orange organic dye after 180 minutes. The wide bandgap of SnO_2 was tuned using GO which showed enhanced photocatalytic performance and had a greater surface area. This shows that doping is an attractive method to enhance the photocatalytic properties of Tin (IV) Oxide.

An Experimental study done by Manikandan et al., 2018fm on Ag activated SnO_2 films for enhanced photocatalytic dye removal against harmful organic dyes prepared by Spray Pyrolysis technique found that the band gap values for the synthesized films are 3.5 for $SnO_2$and 3.2 eV for $SnO_2: Ag$thin films. This reduction in band gap was attributed to the integration of Ag ions into the SnO_2 lattice. The Methylene blue dye degradation test indicated that the rate constant value of SnO_2films is 0.0254min^{-1} and that of $SnO_2: Ag$ films is 0.0193 min^{-1} confirming that $SnO_2: Ag$film exhibits superior photocatalytic activity in comparison to SnO_2 film(Manikandan et al., 2018) indicating that doping a suitable method of improving the photocatalytic efficiency of SnO_2 thin films.

Doyan et al., 2019, investigated the influence of doping on the optical properties of indium-doped Tin (IV) Oxide (SnO_2) thin films using sol-gel spin coating technique. Thermo Scientific's GENESYS UV-Vis Spectrophotometer was used to determine the optical properties of the thin films. From the results of the analysis, indium doped SnO_2thin films transmittance improved from 75 to 96.6% at wavelengths between 300

and 350 nm and the maximum absorbance increased from 3.19 to 4.32 at a wavelength of 300 nm with an increase in doping percentage. It was discovered that Tin (IV) Oxide thin films undergo a drop in energy gap from 3.64 to 3.57 eV as the percentage of doping is increased. Higher doping percentages all contribute to faster electron mobility in Tin (IV) Oxide thin films. The absorbance spectra showed that the absorbance values of thin films increase as the doping percentage increases. Additionally, it was shown that enhanced transmittance happens between 300 and 350 nm in wavelength. The highest peak transmittance values at 350 nm wavelength were 75.0, 78.2, 87.1, 90.6, 94.7, and 96.6%, going in order of lowest to highest doping percentage. This denotes the occurrence of electron motions brought on by photons with energies between 300 and 350 nm. The transmittance graph also seemed constant at wavelengths between 350 and 800 nm. From 2.91 to 2.35 eV, the optical activation energy of the thin films of Tin (IV) Oxide decreased with increasing doping percentage. According to the findings of this research, doped SnO_2thin films showed greater conductivity and less band gap energy and therefore it was concluded, Indium doped Tin (IV) Oxide thin films are of high quality since they have a small energy gap. These properties are attractive qualities of a good photocatalytic material. Hence doping is an effective way of improving the properties of Tin (IV) Oxide thin films.

HA Jalaukhan et al., 2021 prepared and investigated the optical properties and photocatalytic activity of Graphene Oxide-doped Tin (IV) Oxide thin films. They employed spin coating technique to synthesize pure Tin (IV) Oxide (SnO_2) and Tin (IV) Oxide/Graphene Oxide (SnO_2/GO) thin films with varying concentrations of GO (0, 1, 2, 3, and 4 g/ml). All parameters for the reaction were carefully tuned to maintain the excellent crystalline structure of the samples. To achieve this, Pure SnO_2 and SnO_2/GO thin films structural, optical, chemical, and morphological properties were carefully

examined using X-Ray Diffraction (XRD) spectroscopy, Raman spectroscopy, Field Emission Scanning Electron Microscopy (FESEM), and Ultraviolet-Visible (UV-Vis) spectroscopy. The photocatalytic degradation of Methyl Orange under UV light irradiation was also studied. The Graphene Oxide XRD analysis showed that the peak was extremely sharp and high, which indicated that the Graphene Oxide structure had good crystallinity. The photocatalytic activity of the produced samples assessed using Methyl Orange dye under UV light irradiation results showed that increasing the Graphene Oxide concentration enhance the SnO_2 thin film's photocatalytic activity.

2.2.4. Tungsten (VI) Oxide (WO_3) as a Dopant

A review done by Wang et al., 2016 on improving the photocatalytic execution of materials revealed that to overcome issues such as wide band gap, high electron-hole pair recombination rate, and limited efficiency for the utilization of irradiated energy, adjustments such as doping with a metal or metal oxide were applied. He found out that modifiers, such as; Ag^+, WO_3, and W enhance the photocatalytic execution properties of a catalyst by extending the absorption to the visible range(Y. Wang et al., 2016). This indicates that WO_3 is a suitable dopant material.

Koohestani., 2019recovered tungsten in the form of WO_3 nanoparticles from tungsten alloys (W-Ni-Fe) through a chemical method and used them to produce TiO_2/WO_3composites. The composites were assessed utilizing X-ray Diffraction (XRD), Field Emission Scanning Electron Microscopy (FESEM), Brunauera–Emmett–Teller (BET), and DRS analyses. The results showed that as WO_3 increases in amount, the specific surface area and optical band gap are reduced so that the 50%WO_3 compound in the composite brought about the specific surface area of 62.1 m^2/g and an optical band gap of 2.77 eV. He analyzed the photocatalytic execution of the composites by utilizing a

methyl orange dye degradation test under the radiation of UV light. The outcomes indicated that the composite of $TiO_2 - 20\%WO_3$with a specific surface area of 58.2 m^2/g, and band gap energy of 2.94 eV had the highest capability of eliminating the dye. This upgrade in the photocatalytic execution was ascribed to an improvement in light absorption properties and a reduction in the recombination rate of the electron-hole pairs produced by light.

2.2.5 Tin (IV) Oxide doped with Tungsten (VI) oxide (WO_3/SnO_2)

Jwad Abdul-Ameer et al., 2018synthesized Tin (IV) Oxide doped with Tungsten (VI) oxide by thermal evaporation Technique on glass substrates with 1% weight of WO_3 in SnO_2, for gas sensing. Using UV-VIS Spectrophotometer and X-Ray Diffraction (XRD)for characterization they found out that the synthesized films had; a Polycrystalline structure, a reduced band gap of 2.5 eV, an elevated refractive index of 2.51 (Due to high porosity and surface roughness), a smaller grain size in the material (which lowers the activation energy), Tungsten nanocluster over the SnO_2 surface which also reduced the activation energy, Large active surface area, an extinction coefficient of 0.024, an Elevated Transmission (>80%), and a rise in Several oxygen species & the surface states (which reduce surface recombination centers and enhance charge separation efficiency(C. Wang et al., 2015). This confirms that doping SnO_2 with WO_3 is very practical for improving the optical properties of SnO_2such aswide band gap and electron-hole recombination.

Shao et al., 2019synthesized pure SnO_2 and three groups of hollow WO_3/SnO_2hetero-nanofibers with different weights ratios (WO_3 of 0.1, 0.3, and 0.9 wt. %) using uniaxial electro-spinning method combined with calcination. The study investigated gas sensing properties and the working mechanism of WO_3/SnO_2hetero-nanofibers. Characterization

was done using powder X-Ray diffraction (XRD) analysis, Field Emmision Scanning Electron Microscopy(FESEM), Transmission Electron Microscopy (TEM), High Revolution Transmission Electron Microscopy(HRTEM) with energy-dispersive (EDS) detector and X-ray photoelectron spectroscopy(XPS). This study revealed that $WO_3/SnO_2$with different contents of WO_3 show different gas sensing properties, indicating that the optimal dopant proportion is important in constructing WO_3/SnO_2(Stojadinović et al., 2016).

2.3 Theoretical review on SnO_2 and Photocatalyst Thin Films.

2.3.1 Structure of SnO_2

2.3.1.1. Crystallographic structure

Tin (IV) Oxide (SnO_2)cassiterite (rutile phase) has a tetragonal crystallographic structure with space group P42/mnm and lattice parameters $a = b = 4.731$ *Å* and $c = 3.189$ *Å*. Tin Oxde Cassiterite's crystallographic parameters are very close to TiO_2 rutile. As with the SnO_2 rutile structure, It has SnO_6 octahedron building blocks, where each Sn cation is attached to 6 oxygen anions (Ishchenko et al., 2021). Figure 1 below shows an illustration the structure of the cassiterite Unit Cell;

Figure 1

SnO_2cassiterite Unit Cell

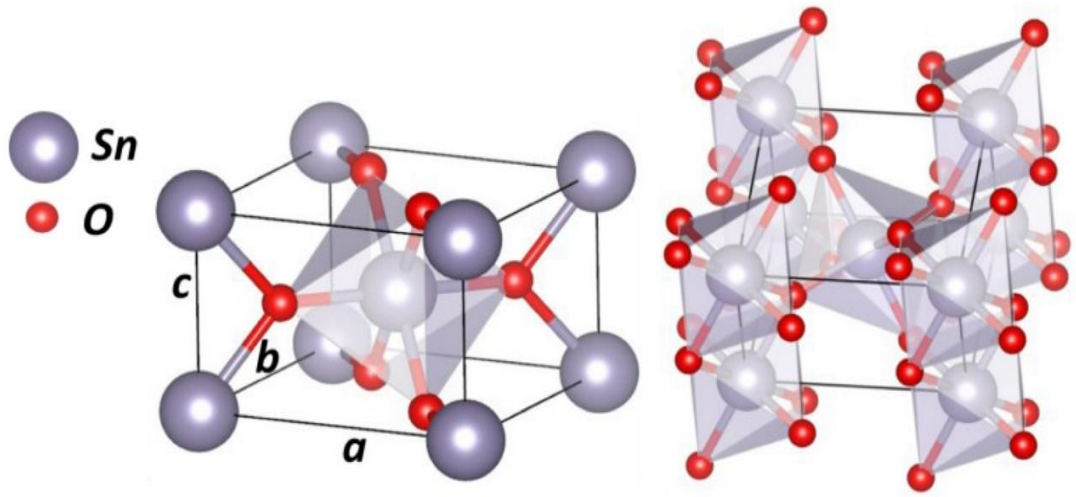

Note: Adapted from (Ishchenko et al., 2021)

2.3.2 Properties and Applications of Tin (IV) Oxide (SnO_2)

Tin (IV) Oxide (SnO_2) is among the fundamental semiconductors in modern technology with a wide band gap, it has a number of applications in materials science and engineering. SnO_2 Thin films are most often recognized as transparent conductors having high electrical conductivities after donor atom doping. SnO_2 has been widely used because of its mechanical stability, resistance to chemical corrosion, low cost of pristine materials and its great optical transparency in the visible region. This semiconductor material has a quadrilateral shape, has an energy band gap that ranges from 3.7 to 4.2 eV(HA Jalaukhan et al., 2021)and has got an n-type conductivity (Sefardjella et al., 2013). Figure 2 illustrates the electronic band gap structure along high symmetry directions.

Figure 2

The Electronic Band Gap Structure of Tin oxide

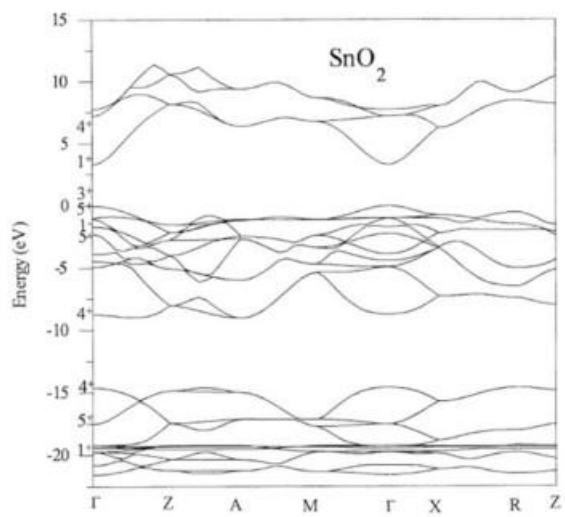

Note: Adapted from (Nabi et al., 2003)

In the SnO_2electronic band structure, the maximum of the valence band (VB) mostly gets contribution from oxygen 2*p* orbitals, while the minimum of the conduction band (CB) is primarily because of tin 4*s* orbitals. Tin oxide has the ability to change stoichiometry on the surface and become SnO, where Sn^{4+}can be reduced to Sn^{2+}. This modification has a significant effect on the surface electronic structure, resulting in the formation of Sn 5s derived surface states and lowering the work function of the materials. The value of the photocatalyst work function can determine the photoactivity of the photocatalysts(Matějová et al., 2014, 2015; Reli et al., 2015). Work function measurements have previously been reported to be a very useful experimental guideline for estimating the energy shift of valence and conduction bands of prepared photocatalysts (Kočí et al., 2016). According to Kočí et al., 2016 research, the material with the lowest work function was found to exhibit the highest photocatalytic performance. The tight connection between the photocatalytic activity and the work function clearly indicates that the electron-donor properties of the catalyst surface, as

measured by the Fermi level position, are the primary factor controlling the reaction rate(Kočí et al., 2016). The work function parameter can also be used to evaluate photocatalysts where surface electron availability is essential in surface-mediated redox processes(Legutko et al., 2013; Maniak et al., 2011; Obalová et al., 2011).

The OGALE research team was credited with writing the first paper on the creation of transparent semiconductor layers made of SnO_2 in 2004. The crystalline structure of the aforementioned layers was notable for its optical transmittance in the visible range, which was about 60%, and its carrier density, which is roughly 1018 cm^3. Since then, researchers have researched the creation of transparent semiconducting magnetic Tin (IV) Oxide with significant impurities due to the increased interest in transparent magnetic semiconductors in recent past(HA Jalaukhan et al., 2021).

Tin (IV) Oxide is an amphoteric colorless solid which shows high transmittance, It is frequently characterized by oxygen vacancies, which improve its characteristics as an n-type semiconductor, it is also characterized by good chemical & thermal stability(Bouras et al., 2014; Yadav et al., 2014). Due to these morphological properties and since its band gap corresponds to activation with photons of a wavelength of 350 nm (UV-A range),It is currently used in numerous fields like transparent electrodes, solar cells, heat mirrors, gas sensors, battery materials, optoelectronic devices and raw material for transparent films (Al-Hamdi et al., 2017; Anandan & Rajendran, 2015; Choi & Park, 2014; B. Liu & Aydil, 2009; J. Liu et al., 2016). The Optical transmittanceand excellent conductivity makes SnO_2 very attractive for optoelectronic, photocatalytic and photovoltaic applications (Bhattacharjee & Ahmaruzzaman, 2015).

2.3.3. Fabrication of Tin (IV) Oxide (SnO_2)

The preparation technique of photocatalytic thin films greatly influences its effectiveness. The sol-gel route is an effective technique to create excellent metal oxide nanostructures as opposed to other physical and chemical methods (Parashar et al., 2020). Sol-gel is one of the simplest, quickest, low-cost technology, and it offers several advantages like controlled stoichiometry, better homogeneity, low processing temperature, high purity, effective control of properties, easy to implement, low cost, high quality, and production of materials with large surface areas (Danks et al., 2016; Parashar et al., 2020; Tseng et al., 2010).

Because of the controlled shape and size exhibited by the obtained products, the sol-gel process has been investigated extensively for producing metal oxide nanostructures for engineering and technological applications. Since Ebelman's preparation of silica gel in 1846, this method has been gradually improved, and sol-gel synthesized materials with excellent magnetic, electrical, optical, thermal, and mechanical propertieshave been used in a variety of applications (Pierre, 2020). Several types of materials, including thin films, nanoparticles, glass, and ceramics, can be produced at a low cost using the sol-gel method. Aside from that, the purity and quality of the yields from the sol-gel process have opened up some new avenues in bioengineering fields such as drug delivery, pharmaceuticals, organ implantation, and biomaterial synthesis(Kianfar & Suksatan, 2021; Thiagarajan et al., 2017). These benefits have enticed researchers and industrialists to use this method extensively over the last few decades. Metal oxides are a type of functional material that can be synthesized using the sol-gel process. Metal oxide can be synthesized in sol-gel at a lower temperature as compared to solid-state reactions(Thiagarajan et al., 2017).

2.3.4 The Sol-Gel Method

This is a wet-chemical technique for the synthesis of nanostructures such as thin films and nanoparticles. In this method, a Sol is obtained through polymerization or hydrolysis reactions, by adding an appropriate solvent to the precursor material to form a homogeneously mixed solution. The prepared sol can then be deposited onto preferred substrates as thin films through spin coating or dip coating, or in the case of the synthesis nanoparticles, the gelation process can be done either through the addition of polymers or condensation of the sol which converts this sol to gel (Thiagarajan et al., 2017). The Figure 3 below shows a schematic diagram of sol-gel processing;

Figure 3

Schematic Diagram of Sol-Gel Processing

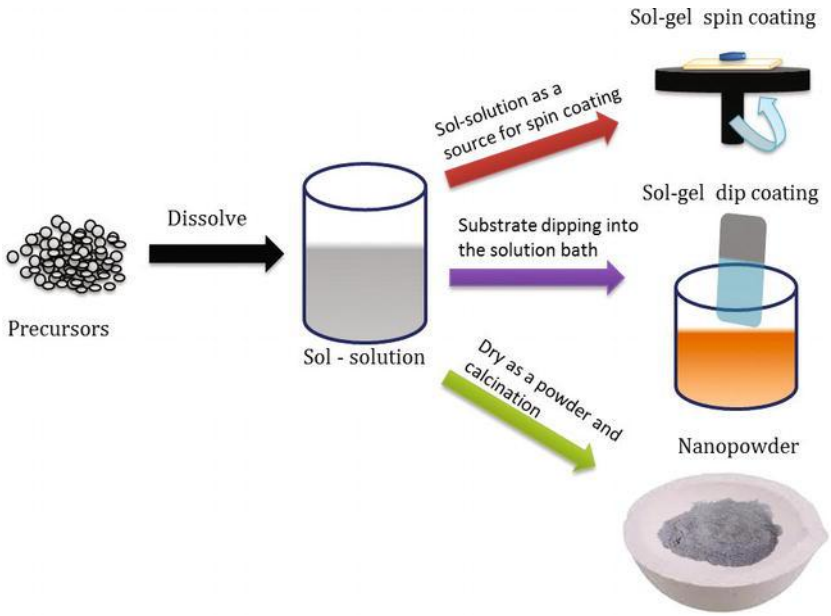

Note: Adapted from (Thiagarajan et al., 2017)

With regard to the deposition of thin films, in comparison to other techniques, the spin coating has key advantages such as; Controlled film thickness, low operation cost, uniformity, rapidness and the capability of easily scaling up (Chaudhary, 2021; Paras & Kumar, 2021). It involves three significant stages; solution dispensing, spinning & thinning, and solvent vaporization as shown in figure 4 below. The spinning draws the

liquid coating into an even covering and then vaporizes to leave the required material on the substrate in a uniform distribution. The rapid drying caused by the high spin speeds and airflow results in great consistency at both the macroscopic and nano length scales (Chaudhary, 2021). Spin coating parameters that affect the thickness of the film are; the rotation speed and acceleration of the spinning plate (Boudrioua et al., 2017).Other parameters that play a very essential role during thin film deposition by spin coating process are the nature of the solution, the nature of the substrate, solution dispensing, and the spin coating duration (Chaudhary, 2021).

Figure 4

Schematic Diagram of Spin Coating

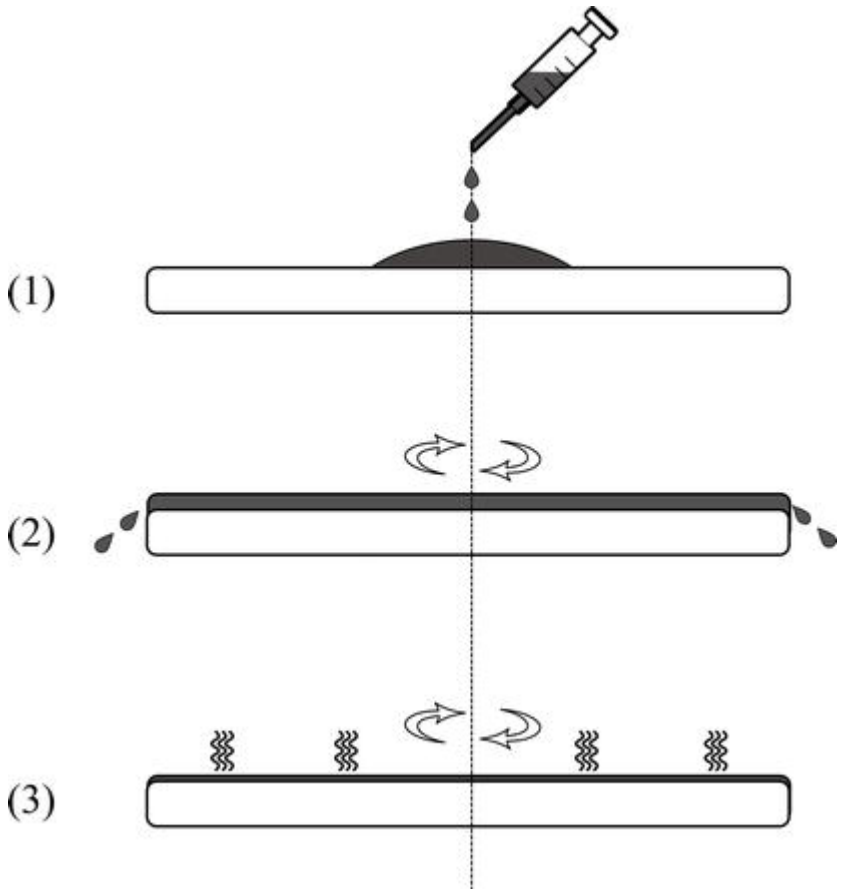

Note: Adapted from (Chaudhary, 2021)

Spin Speed: According to Chaudhary., 2021; Spinning speeds dictate the range of thicknesses that a particular solution may attain. The amount of centrifugal force

provided to the fluid, as well as the speed and turbulence of the air that is directly above it, are all affected by speed. Because of the impact of centrifugal force, the deposited solution flows radially once the substrate starts spinning and excess fluid spins off the substrate. The fluid continues to thin more until the amount of centrifugal force is equal to the viscosity. Even though the spin coating process is split into three steps, the time between them is not always precisely defined. Spin coating generally readily forms a rather uniform thin film from around 1000 rpm and above.

The nature of solution: A number of crucial requirements must be met by the source substance and solvent employed in the spin coating process, which include stability in air at ambient temperature as well as being less toxic. The spin time and spin speed necessary to obtain the desired thickness are determined by many solution factors such as viscosity, density, solvent evaporation rate, concentration, and surface tension.(Chaudhary, 2021). As a result, the nature of the precursor materials used to make the spin coating sol solution should be evaluated to ensure the prepared sol has the required properties.

The nature of substrate: The substrate material has an impact on the overall quality of the produced film. Generally, the substrate has to be chemically and thermally resistant to the coating solution in order to tolerate the subsequent curing or heat treatment. To guarantee comprehensive substrate coverage during dispense, a surfactant is sometimes added to the formulation, or the substrate is changed to promote adequate wetting. The substrate surface, for example, might shift from hydrophobic to hydrophilic based on the nature of the fluid (Mouhamad et al., 2014).

Solution Dispensing: Solution dispensing is the act of applying the fluid on the substrates. An important consideration when introducing the sol solution on to the substrate is whether static or dynamic dispense deposition process is used. In static dispense procedure the spinning process begins and rapidly raised to the appropriate speed, the static dispense process typically covers the whole substrate or the active section of the substrate before spinning. (Chaudhary, 2021).

In the dynamic dispense, the substrate is spun and allowed to attain the necessary speed before the liquid is introduced at the substrate's center. The centripetal force drags the liquid farther from the middle of the substrate through the entire surface before it dries.(Chaudhary, 2021).

Spin Coating Duration: This is the amount of time it takes for the spin coating to occur. Most conventional spin coating techniques maintain the substrate rotating till the film is totally dry, which is determined mostly by the boiling point of the solvent plus vapor pressure under ambient conditions. For most solvents, 30 seconds is generally sufficient. Higher boiling point solvents, on the other hand, may take substantially longer to dry, hence solvents are typically employed as additives or in combination with extra drying operations. The spin coating method has several factors that cancel and average out throughout the spin phase, giving adequate time to regulate the deposition process by integrating fluid flow as well as solvent evaporation processes to produce an extremely thin coating layer.(Yimsiri & Mackley, 2006). During the evaporation process as spinning continues, the viscosity rises until it is equal to the centrifugal force, at which point the spin time is no longer sufficient to move the solution. Here, increasing the spin time has no discernible effect on film thickness. This can take anywhere between 10 seconds and 1 minute (Chaudhary, 2021).

2.3.5 Post deposition Heat Treatment

Annealing is a heat treatment process that alters a material's physical and chemical characteristics. Many important applications of SnO_2 depend on its electrical, structural and optical properties. The fabrication method and heat treatment significantly impacts material's properties (Aghgonbad & Sedghi, 2018) and hence their technical applications, such as water purification through photo degradation, and solar cells (Mahdi et al., 2022; Praveen & Ojha, 2014; Yousefi et al., 2016, 2017, 2019; Yousefi, Alshamsi, et al., 2021; Yousefi, Ghanbari, et al., 2021; Yousefi, Sobhani, et al., 2021). Some of the optical properties influenced by Annealing Temperature are absorbance, transmittance and optical band gap. Annealing process has been used in research to improve optical, electrical and structural properties of deposited thin films. In some semi-conductors thin films, increase in the annealing temperatures, may decrease the optical band gap of films due to reduction of oxygen vacancies in the films(Hsu et al., 2020). The size of crystallites, which has a strong influence on a material's photocalytic performance, is directly related to the temperature in the fabrication process(Armaković et al., 2019; Marotti et al., 2006; Nandiyanto et al., 2017; Sharma et al., 2014).Typically, annealing is used to increase the crystallinity of substances or shift their crystal structure from an amorphous to a crystalline state(Abd-Elnaiem & Hakamy, 2022), this improvement in crystallinity increases both carrier concentration and Hall mobility reducing resistivity of the material, therefore increasing conductivity (Minami & Miyata, 2008). Improved crystallinity may also lead to a decrease in band gap (Yıldırım et al., 2012). This improvement in properties, makes the films high quality for applications in optoelectronic devices and other applications (Doyan et al., 2019).

2.3.6 Working Mechanism of a Photocatalyst

When solar energy is illuminated on photocatalytic material (photocatalyst), photons are absorbed by it. A photon with an energy equal to or higher than the semiconductor band gap will excite electrons (e^-) from the valence band to the conduction band, generating holes (h^+) in the valence band. These generated carriers (e^-, h^+) migrate catalyst's surface, and since they are in contact with water (H_2O) and oxygen molecules (O_2), they participate in redox reactions to induce the formation of hydroxyl radical ($OH^{\cdot}$) and superoxide Anion ($O_2^{\cdot-}$). The Super Oxide Anion and the hydroxyl radical produced further participate in degrading organic pollutants to harmless by-products like carbon (IV) oxide and water as shown in figure 5 below. Finally, clean water free from pollutants is obtained. The following equations summarize the mechanism.

Activation reaction; $SnO_2 + hv \rightarrow h^+ + e^-$ (2.1)

Oxidation reaction; $h^+ + OH^- \rightarrow OH^{\cdot}$ (2.2)

Reduction reaction; $e^- + O_2 \rightarrow O_2^{\cdot-}$ (2.3)

Organic pollutants + $O_2^{\cdot-}$ (or$OH^{\cdot}$) $\rightarrow CO_2 + H_2O$ (2.4)

Figure 5

Working Mechanism of SnO_2 Photocatalytic Material

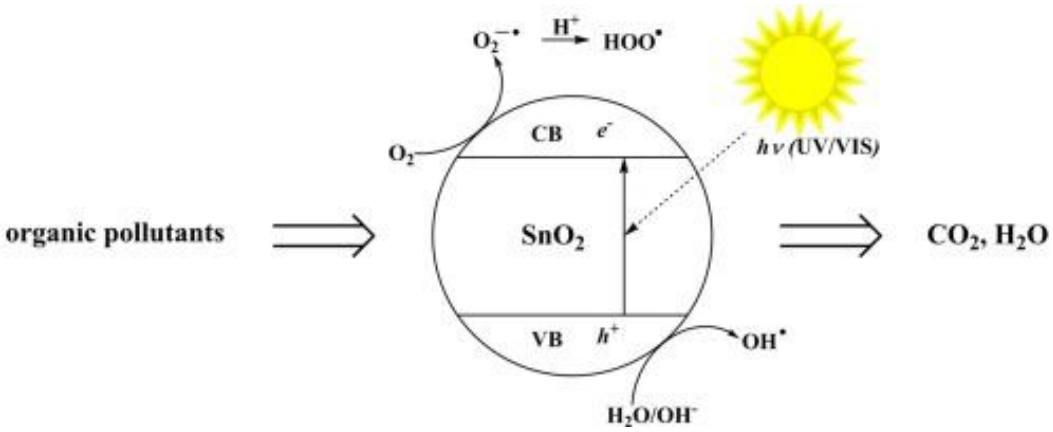

Note: Adapted from (Al-Hamdi et al., 2017)

The activation of e- and h+ is determined by the band gap energy in the photocatalyst between VB and CB(Peiró et al., 2001). Also the acceptable wavelength of the light absorbed to induce the e- and h+ and transferred energy are determined by the band gap (De Wijs & De Groot, 1999).

The chemical reaction that takes place between adsorbed reactants is a concentration-dependent process where a greater concentration produces a quicker reaction and a uniform quantity of the reactant is removed per unit time. In this situation, the degradation kinetics are first-order kinetics, as illustrated byGajbhiye., 2012, photocatalytic dye degradation functions in accordance to this type of kinetics.

In first-order kinetics, the data obtained is expressed in an integrated form. The change in concentration of a reactant A is expressed as;

$$\frac{-d[A]}{dt} = k_c[A] \qquad (2.5)$$

Rearranging equation 2.5 gives;

$$\frac{d[A]}{[A]} = -k_c dt \qquad (2.6)$$

Integrating equation 2.6 we obtain;

$$ln[A] = -k_c t + C \qquad (2.7)$$

When t=0, $[A] = [A_0]$

So that;

$$ln[A_0] = -k_c(0) + C \qquad (2.8)$$

$$C = ln[A_0]$$

(2.9)

This yields;

$$ln[A] = -k_c t + ln[A_0]$$

(2.10)

$$ln[A] - ln[A_0] = -k_c t \quad (2.11)$$

$$ln\frac{[A]}{[A_0]} = -k_c t \quad (2.12)$$

Equation 2.12 is the integrated form of the first-order equation normally referred to the rate law of first-order kinetics. Where, $[A_0]$ is the initial concentration, $[A]$ is final concentration, t is time for reaction and k_c is rate constant obtained by calculating the gradient of a plot of $ln\ A/A_0$ versus time. This is used to quantify the photocatalytic activity of a material.

2.3.7 Photocatalytic Degradation Efficiency Limits

There are a few optical and structural drawbacks that limit the photocatalytic potential of a material. Firstly is a wide bandgap, because of this, light absorption is only permitted for photons with higher energy than the respective optical bandgap energy, thus it limits the use of classical photocatalysts to the UV range of sunlight. This means that only 3-4% of the solar spectrum is involved in a photocatalytic degradation reaction (Ishchenko et al., 2021).

Secondly is the tendency for some electrons and holes to recombine (a few nanoseconds), which reduces the likelihood for them to take part in photocatalysis hence limiting their efficiency(Ishchenko et al., 2021).

2.3.8. Doping of a Photocatalyst

In photocatalysts, doping has been utilized to enhance performance (M. Sun et al., 2019; Y. Wang et al., 2016). This approach involves direct modification of the band gap structure by generating additional energetic levels, to extend the light absorption and also generate trap sites of carriers to avert fast recombination (Ishchenko et al., 2021). Doping increases the charge separation and lifetime of a hole, hence reducing electron-hole pair

recombination and improving photocatalytic execution(Karouei & Moghaddam, 2019; Koe et al., 2020; Trochowski et al., 2019). Doping also incorporates impurity levels into the catalyst's band gap. These levels may be close to the conduction and valence band margins, overlapping with band states and so narrowing the band gap. The impurity integration in the metal-oxide lattice may as well create oxygen vacancies which might be responsible for the photocatalytic efficiency improvement (Ishchenko et al., 2021).

The photon-generated electrons move from more negative to less negative Fermi energy in the conduction band (CB) to avert charge recombination, while holes flow from more positive to less positive Fermi energy in the valance band (VB). Effective charge separation can also be obtained, for instance; WO_3 as a dopant; WO_3 (E.g. = 2.8 eV) can work as an electron-accepting species in the presence of light, which is favorable for producing electron-hole pairs and for improving photocatalytic activity. Doping parameters that affect a material are; dopant concentration and dopant nature (Y. Wang et al., 2016).

2.3.9 Morphological Properties of Photocatalyst Thin Films

The surface morphology of a photocatalyst plays an important role in the photocatalytic activity of a material(Pascariu et al., 2019).The most criticalfactors affecting photocatalytic activity are; surface area, surface area to volume ratio, grain size, and crystallinity regardless of the material(Pascariu et al., 2019). Photocatalytic chemical reactions occur on the surface, therefore increase in the specific surface area ought to improve the efficiency of the process because larger contact area are exposed to the reagents (Ishchenko et al., 2021). Charge-carrier separation can also be improved by controlling the morphology of the photocatalyst(Molinari et al., 2020).

Surface roughness and porosity of thin films are factors that also affect the efficiency of a material. The presence of open pores in some semiconductors can permit the diffusion of the reactants into the photocatalyst material increasing their efficiency. Ramírez-Santos et al., (2012)carried out research on the enhanced photocatalytic activity of titanium dioxide films via polyethylene glycol modification. They discovered that using polyethylene glycol as a polymeric fugitive agent in the fabrication of titanium dioxide films by sol-gel method producing porous, thin films. By using methyl-orange photo-oxidation tests it was determined that the porosity of the films increased their photocatalytic activity. They also found out that increasing the number of layers (from 1 to 5) in the porous Titanium dioxide film increases its photocatalytic response if the generated pores are open, i.e. interconnected, allowing reactants and products to diffuse.

2.3.10 Structural Properties

Structural properties of like the degree of crystallinity and crystal sizes influence the photocatalytic execution of the prepared material(Cheng et al., 2010; Nandiyanto et al., 2020). Crystal structure helps to calculate the crystallite sizes through the Debye-Scherer formula given by;

$$D_{(mm)} = \frac{k\lambda}{\beta\cos\theta} \tag{2.13}$$

Where k is the dimensionless shape factor with a value close to unity, λ is the wavelength of X-ray radiation, β is the full width of half maximum peak (FWHM) and θ is the Braggs' angle in radians. Nandiyanto et al., (2020)who investigated the Correlation between crystallite size and photocatalytic performance of Tungsten (VI) Oxide (WO_3) particles they found out that a raise in the crystallite size has a direct impact to the improvement in the photocatalytic rate of the particles. The results showed that crystalline WO_3 particles had better photocatalytic rate than the particles in amorphous

state. Hence concluding that larger crystal size has strong correlation to the improvement in photocatalytic performance of materials, which is in agreement with similar studies by (Sharma et al., 2014)and (Armaković et al., 2019).

2.3.11. Optical Phenomena in Photocatalyst Thin Films

2.3.11.1. Thin Films Optics

This is the study of a material's optical characteristics and how it responds to electromagnetic radiation incident on it. Photons incident on a semiconductor's surfacewill be either reflected from the top surface, absorbed in the material, or transmitted through the material. The sum of absorptance A(λ), reflectance R(λ), and transmittance T(λ) is Unity (Holden et al., 1997).

$$A(\lambda) + R(\lambda) + T(\lambda) = 1 \quad (2.14)$$

Where; $A(\lambda) = \frac{I_A}{I_0}, R(\lambda) = \frac{I_R}{I_0}, T(\lambda) = \frac{I_T}{I_0}$

$I_0$is the total intensity of incident radiation on the surface, I_A, I_R, and I_T is the intensity of the light absorbed, reflected, &transmitted respectively.

In absorption, the intensity of light I of the radiation is expressed as; (Pankove, 1975)

$$I(z) = I_0 e^{\frac{-2\omega k}{c} z} \quad (2.15)$$

Or

$$I(z) = I_0 e^{-\alpha z} \quad (2.16)$$

Where z is the distance in meters moved by the radiation in the absorbing medium, and $\alpha(\lambda)$ is the absorption coefficient expressed as;

$$\alpha(\lambda) = \frac{2\omega k(\lambda)}{c} \quad (2.17)$$

Where $\omega$is the frequency of the radiation, c is the speed of light, and $k(\lambda)$ is the extinction coefficient responsible for absorption.

From the transmission data the absorption coefficient (α) can also be determined using the relationship;

$$\alpha = \frac{ln\frac{1}{T}}{t} \qquad (2.18)$$

Where t is the film thickness, T is the transmittance andln is the Natural Logarithim.

2.3.11.2. Absorption Coefficient

The absorption coefficient spells out how far light of a specific wavelength may penetrate before being absorbed into a material. It is influenced by type of material, the preparation procedure, the surface morphology, and the wavelength of the incoming radiation. Light is only poorly absorbed in a material with a low absorption coefficient, and if the material is thin enough, it might appear transparent to that wavelength (Educator, 2022). Its study provides data concerning electronic states in high-energy areas and atomic vibrations in low-energy regions.

The absorption coefficient in semiconductors has a sharp edge where radiation energy below the band gap is not strong enough to move an electron from the valence to the conduction band, resulting in no light absorption. The possibility of absorbing a photon is determined by the likelihood of a photon and an electron interacting in such a way that they go from one energy band to another. The absorption coefficient for a photon with an energy near to the band gap energy is relatively low because only electrons at the edge of the valence band are excited, resulting in less absorption. However, with a high-energy photon, both electrons on the valence band edge and those with energies close to the band gap are exited. As a result, more electrons interact with the radiation, resulting in greater absorption. (Chebwogen, 2019; Chebwogen et al., 2019).

According to Tauc's relation, the absorption coefficient relates to the energy of light quanta;

$$\alpha = \frac{(h\nu - E_g)^n}{h\nu} \quad (2.19)$$

Where h is the Planck's constant (6.626 x 10^{-34} Js), ν is the frequency of the radiation, and n provides the kind of transition, which might be either direct or indirect. In the case of a direct band gap, $n = \frac{1}{2}$substituting for n in equation 2.19 and rearranging gives;

$$(\alpha h\nu)^2 = h\nu - E_g \quad (2.20)$$

Therefore, a plot of $(\alpha h\nu)^2$ against $h\nu$will produce a curve with a straight line at a certain portion. Extrapolation of the straight section of the graph to the point of $(\alpha h\nu)^2 = 0$ gives the energy band gap, E_g.

2.3.11.3. Optical Constants Refractive Index and Absorption Coefficient

Knowledge of the optical constants *n* and *k* with respect to photon energy is necessary when investigating thin film optical properties. A table of *n* and *k*can be used to predict the material's response at each wavelength (Gaspari, 2018). Simple dielectric function models aid in the realistic modeling of optical spectrum and enable parameter fitting to acquire the required information. Examples of the models for simulation are as follows; OJL interband transition model, Drude model for free carriers, KIM extended oscillator, Brendel extended oscillator model, Harmonic oscillator, and Tauc- Lorentz interband transition mode (Chebwogen, 2019; Chebwogen et al., 2019; Sap et al., 2011). The model employed is determined on the substance being investigated and the spectral range. The simulation model utilized determines which parameters must be adjusted.

2.3.11.4. Optical Band Gap

The band gap (E_g) is the energy required to shift an electron from the valence band into the conduction band, given in electron volts (eV). In the case of semiconductor absorption, a rise in absorption occurs at a certain energy value as a result of electrons being stimulated from the valence to the conduction band. The band gap energy is the smallest amount of energy that stimulates electrons confined in the valence band to move freely inside the crystal lattice. These electron transitions in semiconductors can be either direct or indirect (Chebwogen et al., 2019; Patterson & Bailey, 2010). In a direct bandgap semiconductor, the top of the valence band (VB) and the bottom of the conduction band (CB) occur at the same value of momentum as shown in Figure 6.

Figure 6

Diagram Illustrating Direct Band Gap transition

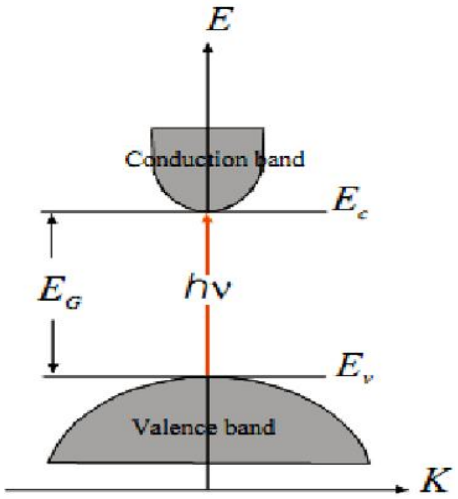

Note: Adapted from (Rathod, 2014)

In an indirect bandgap semiconductor, the maximum energy of the valence band (VB) occurs at a different value of momentum to the minimum in the conduction band (CB) energy as shown in Figure 7 below.

Figure 7

Diagram Illustrating Indirect Band Gap Transitions

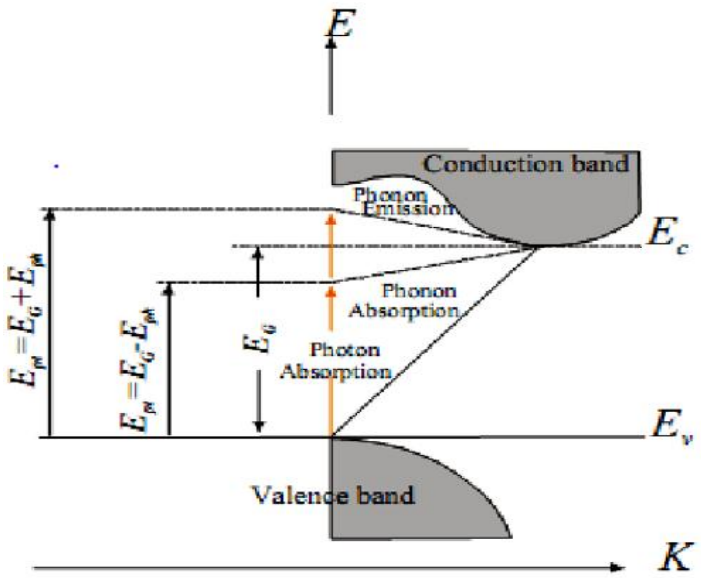

Note: Adapted from (Rathod, 2014)

Direct band gap materials have been claimed to be more efficient than indirect band gap materials for a variety of applications due to their higher absorption coefficient when compared to indirect band gap semiconductors. Direct band gap materials often provide for the lowest energy transfer from the valence to conduction bands without affecting the wave vector (k). However, for electron transitions to occur in an indirect band gap material, the wave vector must be modified with phonons. Therefore, as a result Tin (IV) Oxide thin film direct band gap, it is appropriate for photocatalytic applications.

2.4 Conceptual Framework

The framework in figure 8below depicts the relationship that exists between independent and dependent variables. Independent variables such as; the dopant proportion, annealing time, annealing temperature, spin coating parameters and film thickness are factors that ultimately influence the optical and morphological, and structural properties of a material such as; Band gap, Charge separation, absorbance, optical constant scrystallinity, and

crystallite size. These properties ultimately influence the photocatalytic performance of materials (Rate Constant :K_c).

Figure 8

Conceptual Framework

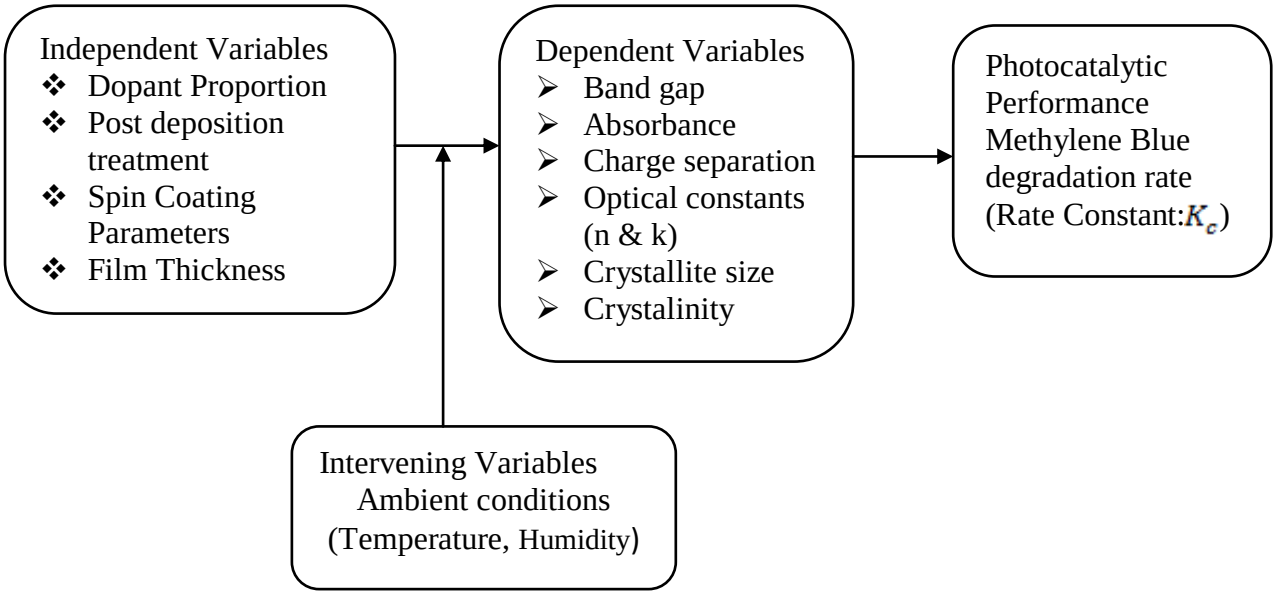

Source: Author, (2023)

2.5 Summary and Research Gap

Although much research has been done on Tungsten (VI) Oxide (WO_3) and Tin (IV) Oxide (SnO_2), there is limited information on the combination of these two materials through doping for photocatalytic application. The table 2 below gives a summary of the research gaps identified.

Table 2

Research Gap

Authors	Research	Key Findings	Research Gap
Al-Hamdi et al., (2017)	Tin dioxide as a photocatalyst for water treatment: (A review).	>The applicability of the pure SnO_2 for water treatment is limited because of the high activation energy of the compound and swift recombination rate of the photogenerated electrons and holes. >To enhance the photocatalytic activity, the Electron-Hole-Pair recombination needs to be addressed through doping the material.	✓A need to find a suitable dopant material to enhance photocatalytic performance ofSnO_2
Azim et al., (2021)	$GO - SnO_2$Nano composite for Photodegradation of Methyl Orange Under Direct Sunlight Irradiation and Mechanism Insight (Experimental study)	>Modifying Tin (IV) Oxide by doping can narrow its wide bandgap and enhance the photogenerated charge separation. >The synthesized Graphene Doped Oxide-Tin Oxide nanoparticles showed an efficient photodegradation (~94%) for Methyl Orange organic dye after 180 minutes. >wide bandgap of SnO_2 was tuned using GO which showed enhanced photocatalytic performance with greater surface area compared to pure SnO_2	✓A Need to modify and synthesize SnO_2 thin film through doping it with other oxides to study how they influence its photocatalytic activity.
Jwad Abdul-Ameer et al., (2018)	Comparative NO_2 Sensing Characteristics of $SnO_2:WO_3$ Thin Film Against Bulk and Investigation of Optical Properties of the Thin Film. (Experimental study)	>The synthesized $SnO_2:WO_3$ had; ✓ A polycrystalline structure ✓ A reduced band gap of 2.5 eV ✓ An Elevated refractive index of 2.51 (Due to high porosity and surface roughness) ✓ Tungsten nanocluster over the SnO_2surface which	✓ Lack of research on the Application of WO_3/SnO_2 prepared by sol-gel method for photocatalytic water

		reduced the activation energy ✓ A Large active surface area ✓ An extinction coefficient of 0.024 ✓ An elevated Transmission (>80%) ✓ A rise in oxygen species and the surface states	treatment ✓ A need for further analysis on morphological properties using SEM and TEM for photocatalytic water treatment
Y. Wang et al., (2016)	The Application of Nano- TiO_2 Photo Semiconductors in Agriculture. (A review)	>To overcome wide band gap, high EHP recombination & Poor light absorption, doping is applied. >Metals or metal oxide doping extends the TiO_2 absorption to the visible range >Modifiers, such as; Ag^+, WO_3, and W, improve photocatalytic execution of TiO_2 >WO_3 (E.g. = 2.8 eV) can work as an electron-accepting species in the presence of visible light	✓ Lack of research on the influence of WO_3 as a dopant on SnO_2 for photocatalytic water treatment
Shao et al., (2019)	Hollow WO_3/SnO_2 Hetero-Nanofibers: Controlled Synthesis and High Efficiency of Acetone Vapor Detection. (Experimental Study)	>Heterojunctions with different contents of WO_3 showed different gas sensing properties >Optimal dopant proportion is important in constructing heterojunctions	✓ Need for further studies on the optimal dopant proportion for an efficient WO_3/SnO_2 for photocatalytic water treatment

CHAPTER THREE

RESEARCH DESIGN AND METHODOLOGY

3.1 Introduction

This chapter presents the research design, materials, and methods that were used for the preparation, characterization and photocatalytic activity study of pureSnO_2 and WO_3/SnO_2thin films.

3.2. Research Design

This was an experimental study and was carried out in the laboratory at room temperature with the magnetic stirring rate of the solutions kept constant at within a specific time depending on the solution being prepared. Spin coating of different groups of WO_3/SnO_2 (WO_3 of 0.0, 0.1, 0.3, 0.5, 1.5, 2.0 wt. %) was done at 1200 rpm for 30 seconds. Characterization and data analysis involved the use of UV-VIS spectrophotometer, SCOUT software and X-Ray diffraction (XRD). The results obtained are presented graphically and discussed.

3.3. Materials

The basic materials used in this work weresodium tungsten dihydrate ($Na_2WO_4.2H_2O$, 99% Merck), nitric (V) acid (HNO_3, 65% Merck), hydrogen peroxide (H_2O_2, 30% Merck), tin (II) chloride dihydrate ($SnCl_2.2H_2O$ Purified from Merck), ethanol (99.9%), methylene blue powder, distilled water, acetone and Helmanex (III) solution.

3.4. Preparation of Thin Films

3.4.1. Preparation of SnO_2 and WO_3/SnO_2precursors (sol solution)

Pure SnO_2 and WO_3/SnO_2sol solutions were prepared using Sol-gel technique according to(Marikkannan et al., 2015; Naseri et al., 2010). In a typical synthesis to prepare WO_3

precursor sol solution, 6 g of sodium tungsten dihydrate ($Na_2WO_4.2H_2O$) was immersed in 30 ml of nitric acid solution (HNO_3) for forty five minutes. After three washes with distilled water, the obtained yellow-greenish precipitate was dissolved in 10 ml of Hydrogen Peroxide (H_2O_2), and 1 ml of ethanol was added to the solution. After 24 hours, it was exposed to light for 2 hours using a commercial 105 W lamp to concentrate the solution. The solution's color changed from colorless to light yellow, and it was stable for a long time. It was then left for 24 h aging.

SnO_2 Precursor Sol solution was prepared by dissolving 0.5 mole of Tin (II) Chloride dihydrate ($SnCl_2.2H_2O$) in ethanol. The prepared solution was magnetically agitated for 5 hours in a closed conical flask and aged for 24 hours at room temperature to improve its viscosity.

The prepared SnO_2 sol was mixed with controlled amounts of WO_3 sol under magnetic stirring for 2 hours to produce six groups of WO_3/SnO_2 (WO_3 of 0.0, 0.1, 0.3, 0.5, 1.5, 2.0 wt. %). The prepared precursor sols were then labeled according to the percentage doping proportion of WO_3 in WO_3/SnO_2 as pure SnO_2, WO_3/SnO_2(0.1%), WO_3/SnO_2(0.3%), WO_3/SnO_2(0.5%), WO_3/SnO_2(1.5%), WO_3/SnO_2(2.0%).

3.4.2 Cleaning of Glass Substrates

The microscope glass slides to be used for thin film deposition were first cleaned in soapy warm water and rinsed before being ultra-sonically treated in warm distilled water for five minutes to remove any particles on the slides. They were then immersed in pure acetone and ultra-sonically treated for five minutes to remove grease and oil stains. After that minerals and metals on the surface of the glass sides were removed by treating them ultra-sonically for 15 minutes in a solution containing a mixture of 2ml Hellmax (III) and

100ml distilled water boiled to about 75°C (almost boiling). Finally, they were removed and thoroughly rinsed in distilled water.

3.4.3. SnO_2 and WO_3/SnO_2 Coating and Annealing Process

Spin coating was used for the deposition process. The prepared sol solutions of SnO_2 and WO_3/SnO_2were transferred into a 2ml syringe and drops of the solution were dispensed onto the cleaned glass slides covering the entire glass slide and then spin coated at 1200 rpm for 30 seconds. After spin coating, the coated glass substrates were then heat treated at 100^{o}C for 10 min to remove any residual organic solvents. The films were then annealed at 500°C for 1 hour in a Carborlite 301 Heating furnace. Figure 9 shows the Laurell 650M Spin Coater that was used in Spin Coating.

Figure 9

A photograph of Laurell 650M Spin Coater

3.5. Preparation of Nanoparticles

To investigate the influence of doping on crystal structure, nanoparticles were prepared since the available X-Ray Diffraction (XRD) equipment was a powder XRD. To prepare the nanoparticles, Aqueous ammonia solution (6 ml.) was added to 30ml of pure SnO_2

and WO_3/SnO_2 sol solutions separately, drop wise under stable stirring. The resulting gel was filtered through vacuum filtration and purified by washing with ethanol and then dried for 5 hours at 100 ºC. The formed nanoparticles were Annealed at 500ºC for 2 hours in a carborlite 301 Heating furnace. Figure 10 below is a summary of the procedure that was used;

Figure 10

Schematic Diagram of the Experimental Procedure that was used

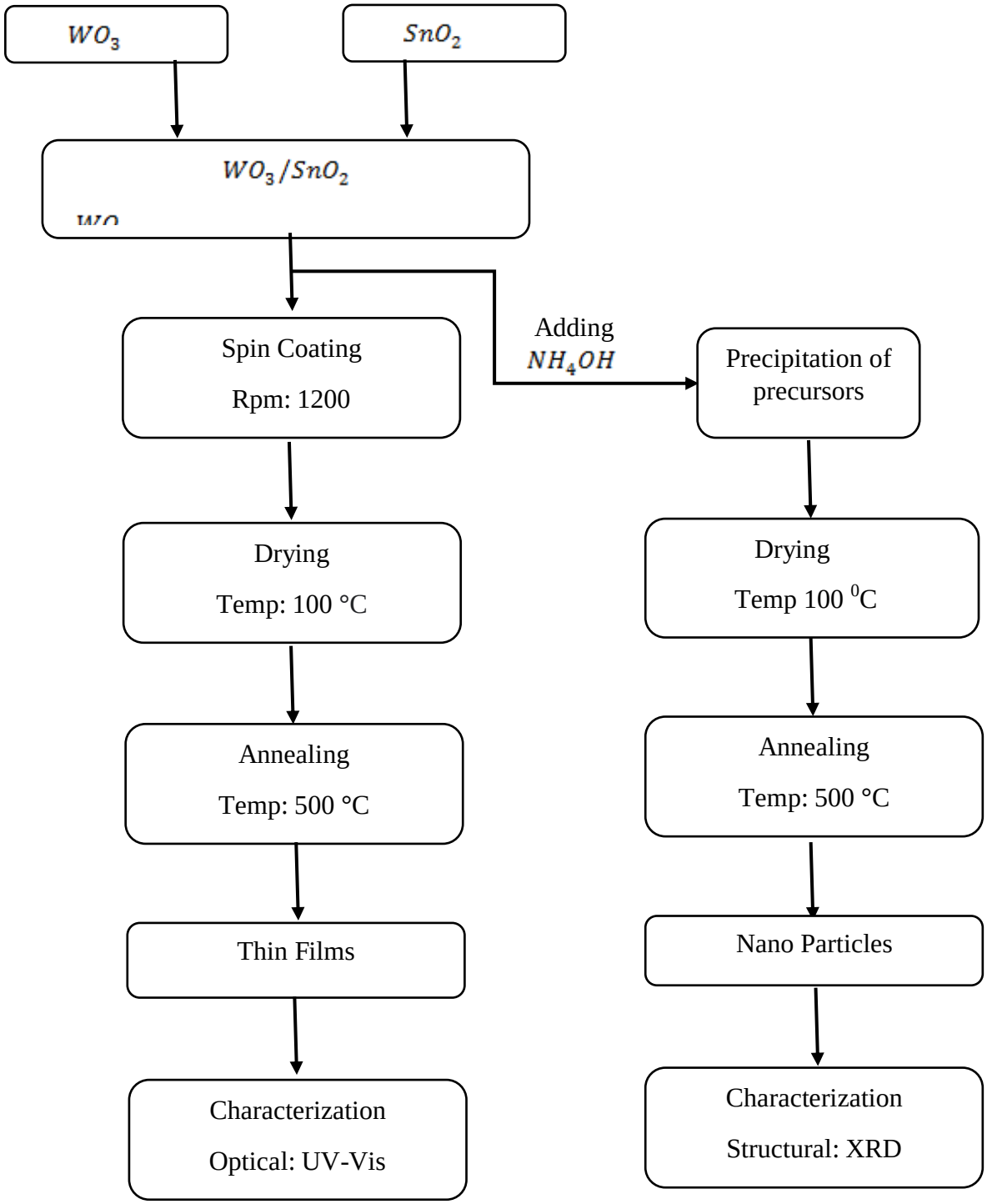

3.6 Instruments used in Characterization of SnO_2 and WO_3/SnO_2.

3.6.1 Optical Characterization

The Shimandzu UV-VIS 2600 spectrophotometer was used to obtain absorbance spectra of the thin films deposited on the glass substrate. The instrument wasfirst switched on when all the sample compartments were empty. Settings of the desired wavelength range, mode typeand the scan speed were made.A cleaned glass substrate was inserted as a reference sample followed by pressing auto zero and then baseline to auto zero the instrument before taking actual measurements. The spectrophotometer was set to measure the absorbance of the films in the range of 200nm to900nm. Figure 11 below displays the UV-VIS spectrophotometer that was used.

Figure 11

A photograph of the Shimandzu UV-VIS 2600 Spectrophotometer

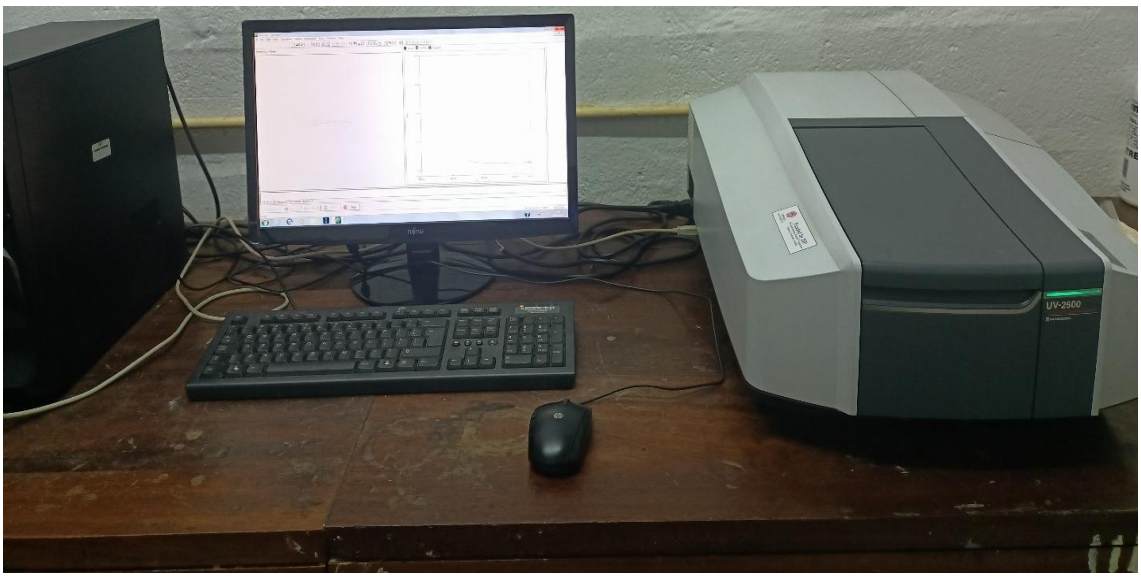

3.6.2 Structural Characterization

The crystal structures of the nanoparticles were determined using X-ray diffraction (XRD, Olympus TERRA-538) with CoKα (λ = 1.7889 Å) radiation at 30.3Kv and 0.006

mA. The samples were analyzed over 20º-55º 2θ with a step size of 0.02º 2θ.Figure 12 below displays the XRD that was used.

Figure 12

A Photograph of the Olympus TERRA-538 XRD

3.6.3 Investigation of Photocatalytic Performance of the Thin Films

The photocatalytic execution of the prepared samples of pure SnO_2 and WO_3/SnO_2 films was tested using the methylene blue dye degradation test under UV light radiation using a system made up of a cabinet and a UV lamp and a magnetic stirrer. The sample was first dipped in 80ml of methylene blue dye solution (3 ppm) in a glass beaker and placed in the dark for 60 minutes to achieve adsorption-desorption equilibrium to be reached, the contents were then moved into the UV cabinet and illuminated for 120 minutes at ambient temperature. To achieve a constant light intensity on the film's surface, the distance between the light source and the film was kept constant. During the photo degradation process, dye sample of 2 ml was taken from the reaction solution at every 30 minutes for absorption studies. Absorbance was measured using the UV-VIS

Spectrophotometer and a graph plotted. The rate of degradation was then assessed by comparing methylene blue degradation rates of pure SnO_2, and WO_3/SnO_2 films.

The pseudo-first-order kinetic model (Gajbhiye, 2012)was be used to quantify the photocatalytic activity of the samples by finding the kinetic rate constant k_c (min^{-1}); According to this model the kinetic rate constant k_c (min^{-1}) is determined by using the relation;

$$ln\left(\frac{C_t}{C_o}\right) = -k_c t \qquad (3.1)$$

Where; C_t is the Sample concentration after degradation time t, C_o is the initial concentration of the sample after adsorption-desorption in the dark and ln is Natural Logarithm. Below is the experimental Set-up that was used for the photocatalytic experiment.

Figure 13

The Experimental Set-Up that was used for the Photocatalytic Experiment

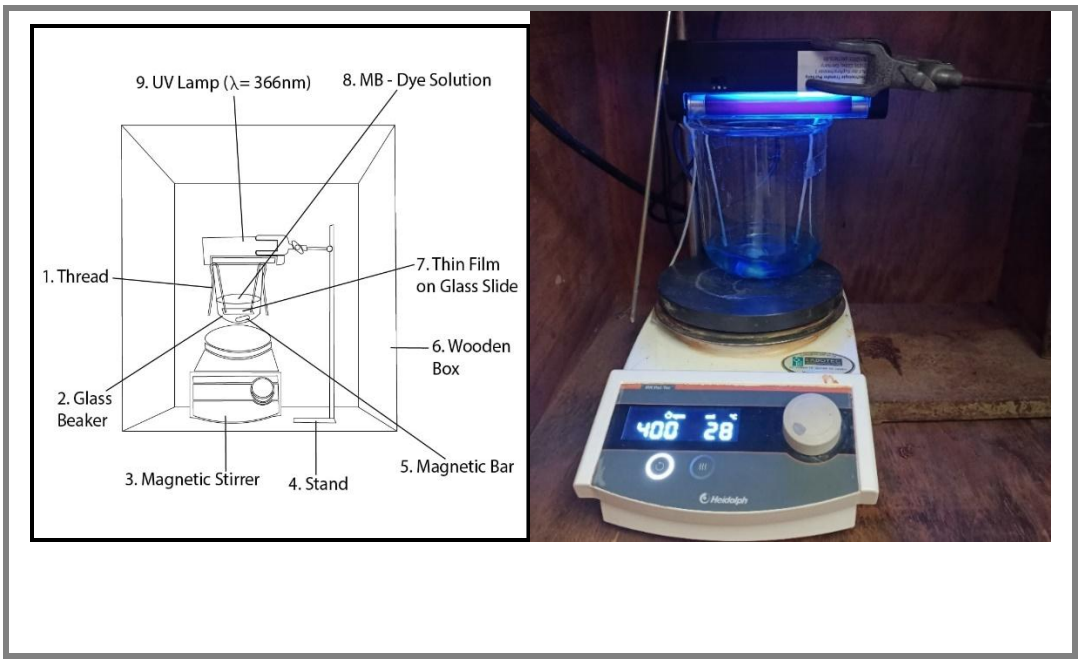

3.7 Data Collection Procedure

A letter from Kabarak University Institute of Postgraduate Studies was obtained at the start of this research work, allowing data collection and report writing. The University of Zambia also provided an affiliation letter, granting the permission of using the equipment in the School of Natural Sciences. An application for a temporary permit from Zambia immigration was made for the duration of the research. Further a KUREC clearance was obtained from Kabarak University Research and Ethics Committee that enabled me obtained NACOSTI research permit, therefore getting the required ethical clearance to proceed with my research work.

3.8. Data Analysis

SCOUT (Theiss, 2002)commercial software was used to analyze data. This software simulates and analyzes various optical spectra such as absorbance, transmittance, reflectance, ellipsometry, and photoluminescence. The program analyzes the measured experimental data by fitting it to simulated data spectra that are either found inside or provided into it. The software is a collection of models, including Classical Drude model for free carriers, Extended Drude model for free carriers, Harmonic oscillator model, Brendel extended oscillator model, Kim extended oscillator model, Leng oscillator model, OJL interband transition model for amorphous materials, Tauc-Lorentz interband transition model for crystalline materials, and User-defined expressions for optical constants (including the option to define Cauchy models).

Optical constant models describe the response of matter to the electric fields of a light wave. The main mechanisms are; acceleration of free charge carriers in conductive materials (free charge carrier absorption), exciting oscillations of bound charges

(vibrational modes), and lifting up electrons from an occupied electronic state to an empty state (interband transitions).

The model to be used in fitting spectra is determined by the material under investigation and the range of the spectrum being employed. Drude, Kim Oscilator, Tauc-Lorentz, harmonic oscillator, and OJL interband transition model (Theiss, 2002)were employed in this work.

CHAPTER FOUR

DATA ANALYSIS, PRESENTATION AND DISCUSSION

4.1 Introduction

This chapter presents and discusses experimental results on the optical and structural properties of SnO_2 and WO_3/SnO_2 thin films. The optical property measured was absorbance. Further the optical constants determined are also discussed, including the refractive index, extinction coefficient and Optical band gap. Structural Properties investigated include Crystallinity and Crystallite sizes. This chapter also includes photocatalytic test results from the methylene blue dye degradation test, as well as how the dopant proportion affected the material's rate constant.

4.2 Results and Discussion

4.2.1 Deposition of Pure Tin (IV) Oxide (SnO_2) and WO_3/SnO_2Thin Films

Thin films of Tin (IV) oxide (SnO_2)andWO_3/SnO_2 (WO_3 of 0.0, 0.1, 0.3, 0.5, 1.5, 2.0 wt.%) films were successfully prepared on a glass substrate, a transparent colorless film formed on its surface. The formation of a colorless transparent film on the surface of the glass substrate confirmed the formation of Tin (IV) Oxide thin film, which resulted from spin coating the sol to the substrates, translating it to the surface of the substrate, and excess liquid spanned off, resulting in the formation of a uniform thin film on its surface. The colorless color of Tin (IV) Oxide (SnO_2)thin films obtained in this study is consistent with those previously reported by(Lee et al., 2013)and (Boshta et al., 2010).

The average film thickness of the fabricated films were modelled using SCOUT software (Theiss, 2002)where the obtained experimental spectra was fitted to the simulated spectra within the software (at a range of 210–900 nm) with suitable optical

model, based on the best fit between experimental and simulated spectra as illustrated in Figure 13 below. The fabricated films had an average thickness of 135.4 nm.

Figure 14

An Illustration of Fitting of the Experimental to Simulated Spectra using the SCOUT Software

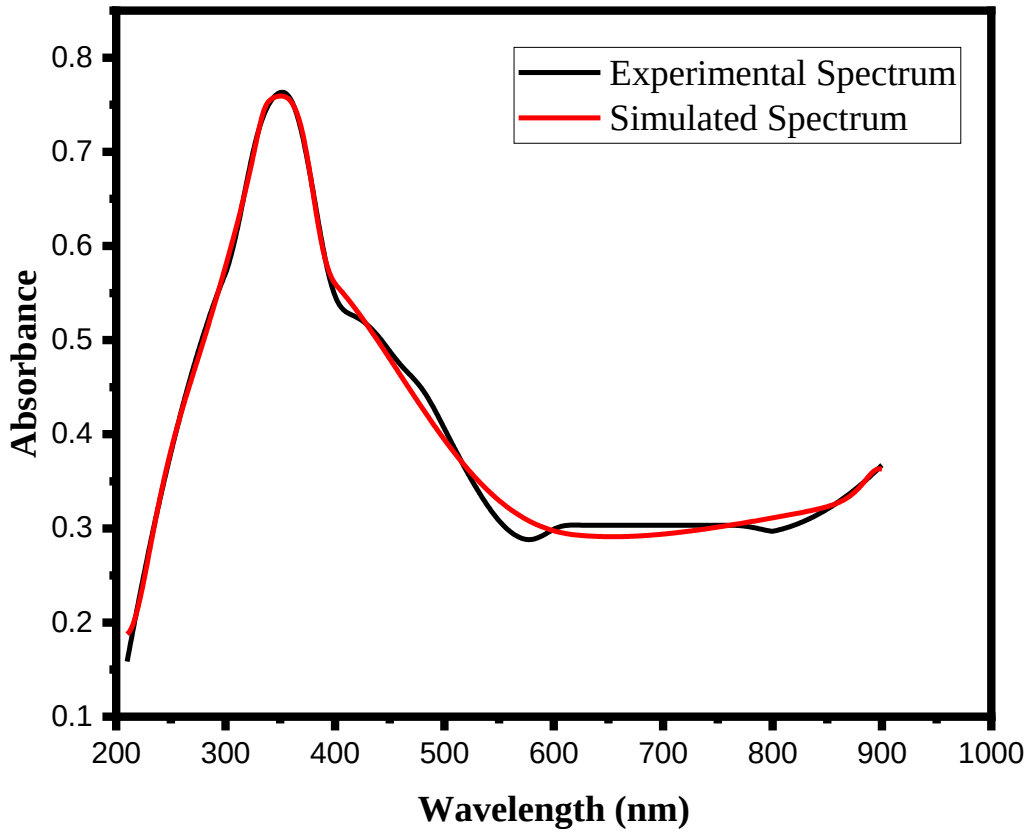

4.2.2 Optical Characterization of the Thin Films

4.2.2.1 Absorbance

The absorption potential of photocatalytic material plays an important role in improving itscapacity to remove pollutants(Yang et al., 2016). Figure 15 below shows, the maximum absorbance of the undoped SnO_2 thin films is in the region (275 nm $\leq \lambda \leq$ 350 nm).This trend is in a good agreement with results that have been reported for pure SnO_2 thin films deposited by Bhagwat et al., 2015 and Doyan et al., 2019. As observed from the spectra there is an increase in absorbance after doping the material. This increase is due to incorporation of WO_3 into SnO_2 which results in increased surface roughness,

causing diffuse reflection and thus an increase in absorbance. In case of photocatalytic effect greater absorption indicates the higher capacity for degradation of pollutants (Islam & Kumer, 2020) because more electron-hole pairs will be produced that drive photocatalytic reactions implying an improvement in the photocatalytic efficiency of the films(Chen et al., 2020). WO_3/SnO_2 (1.5 wt.%) exhibit the highest optical absorbance with a wider absorption range in the visible region. Doping beyond 1.5% instead lowered the absorbance of the films, because dopant proportion exceeding a particular limit instead reduces its absorption (Chebwogen, 2019).

Figure 15

Absorbance against Wavelength for pure SnO_2 and WO_3/SnO_2 thin films with different proportions of WO_3

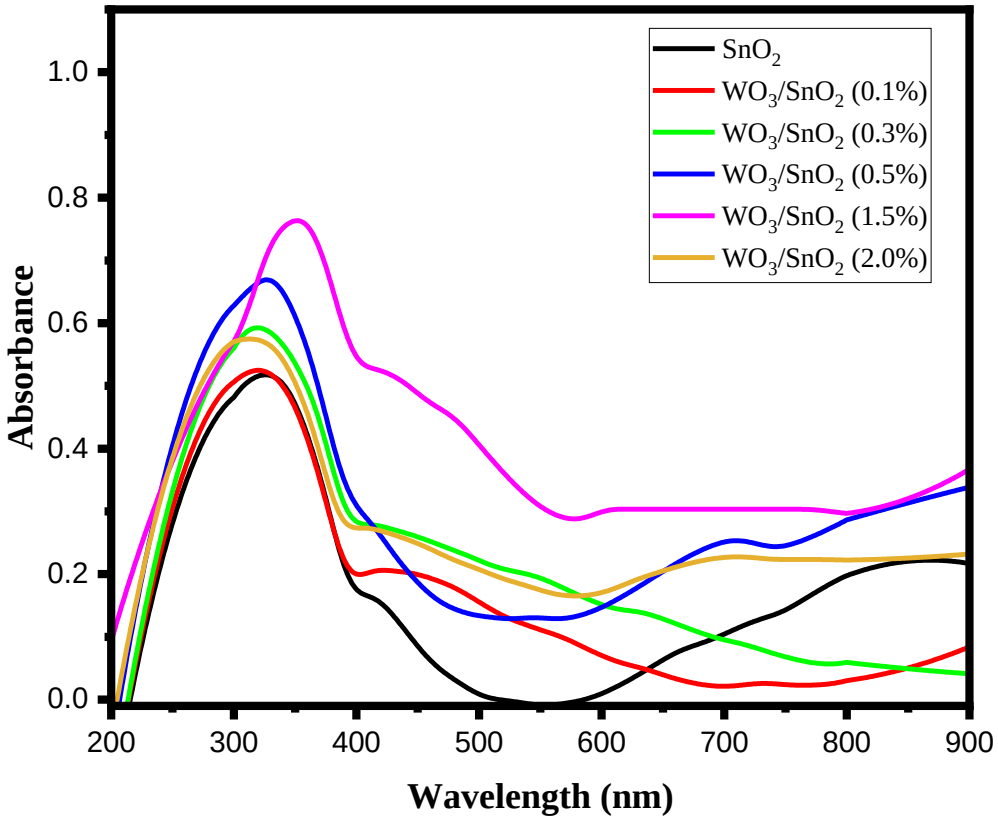

4.2.2.2 Absorption Edge

From the Figure 16 below, the position of the absorption edge of WO_3/SnO_2thin film shifts towards the higher wavelength side. This red shift according to Manikandan et al., 2018indicates a decrease in the band gapwhen doped with a metal or Metal Oxide.WO_3/SnO_2 (1.5 wt.%) exhibits the greatest red shift with a wider absorption range in the visible region. This red-shift can be attributed to a shift in the position of the conduction or valence band, which results in a narrowing of the bandgap and, causing, a red shift at the absorption spectrum's edge (Gao et al., 2019). Doping beyond 1.5% instead caused a blue shift in the absorption edge of the prepared films indicating an increase in band gap beyond the WO_3 (1.5%) dopant proportion.

Figure 16

Effect of WO_3 doping on the Absorption edge of SnO_2 films

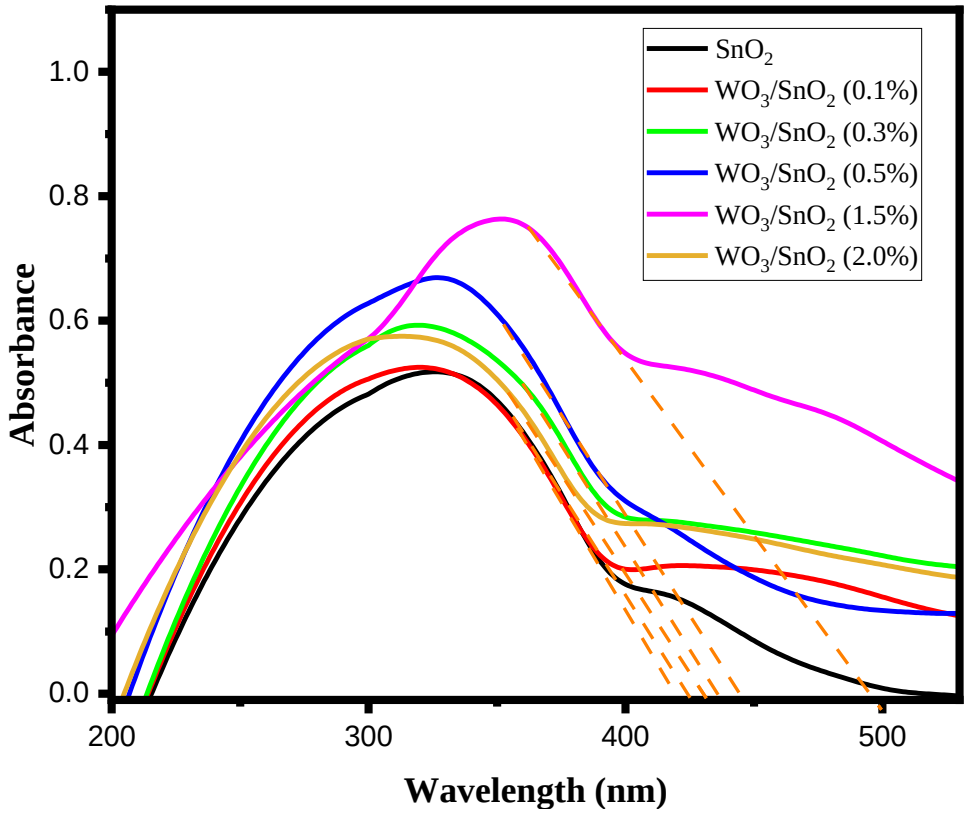

4.2.2.3 Optical Band Gap

The excitation of an electron from the valence band to the conduction band by absorption of photon energy depends on the band gap of the material.

The band gap E_g was determined using Tauc's relationship

$$\alpha h\nu = A(h\nu - E_g)^n \quad (4.1)$$

Where α is absorption coefficient, $h\nu$ is photon energy and A is a constant relation between absorption coefficient (α), and photon energy ($h\nu$). Plots $(\alpha h\nu)^2$against $h\nu$ of pure SnO_2 and WO_3/SnO_2thin films were made, giving curves with a linear parts. Extrapolation of the linear region to the $h\nu$ axis, give the band gaps (E_g) of each film. Figure 17 shows the plot of $(\alpha h\nu)^2$ against $h\nu$ for WO_3/SnO_2 thin films doped at varied WO_3 proportions.

Figure 17

Plots of $(\alpha h\nu)^2$ versus photon energy (hυ) for (a) pure SnO_2, (b) WO_3/SnO_2 (0.1%) (c)WO_3/SnO_2 (0.3%), (d) WO_3/SnO_2 (0.5%) (e) WO_3/SnO_2 (1.5%) and (f) WO_3/SnO_2 (2.0%).

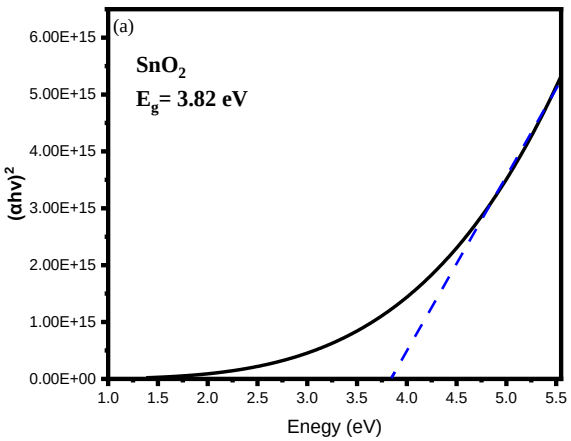

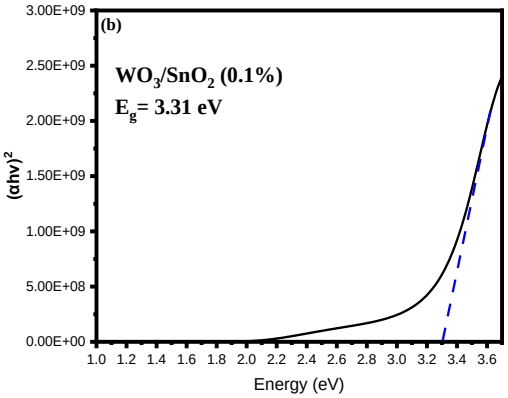
(b)
WO3/SnO2 (0.1%)
Eg= 3.31 eV
(αhν)2
Energy (eV)

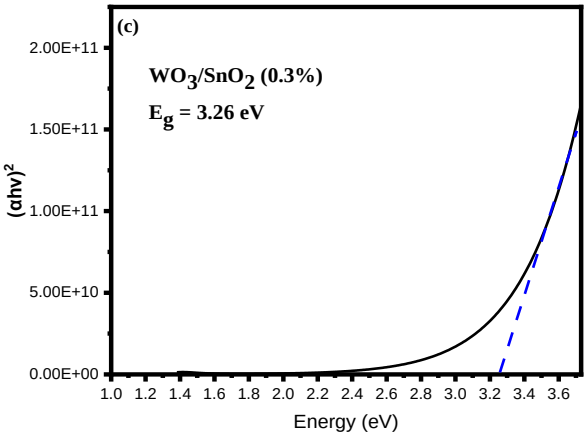
(c)
WO3/SnO2 (0.3%)
Eg = 3.26 eV
(αhν)2
Energy (eV)

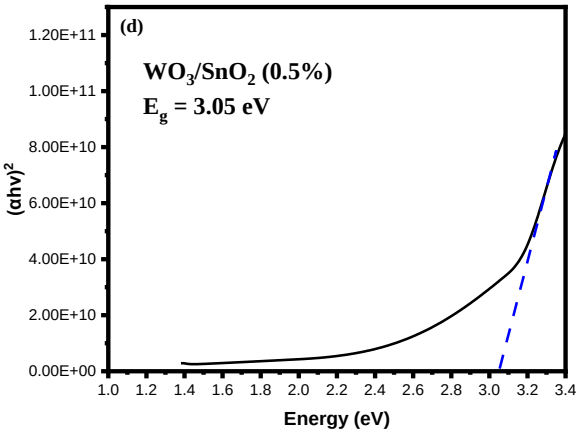
(d)
WO3/SnO2 (0.5%)
Eg = 3.05 eV
(αhν)2
Energy (eV)

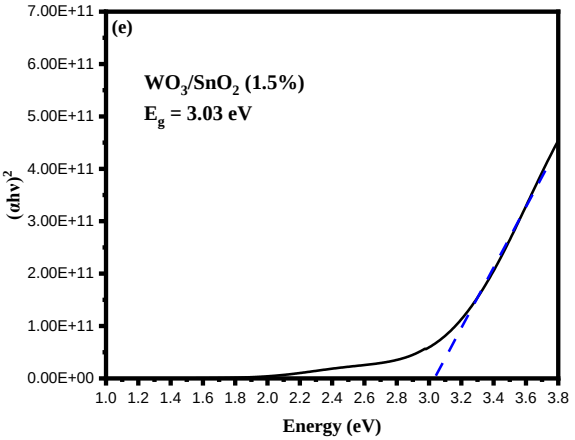
(e)
WO3/SnO2 (1.5%)
Eg = 3.03 eV
(αhν)2
Energy (eV)

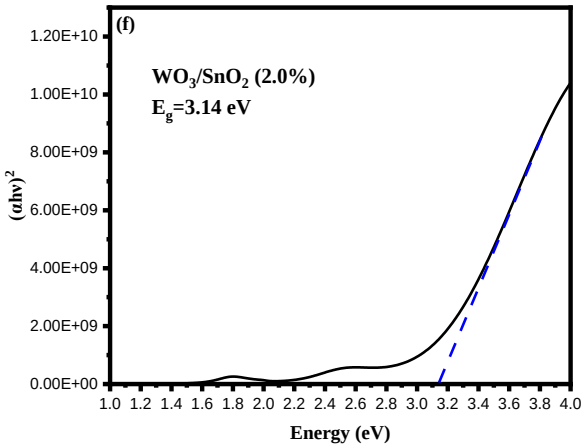

Table 3

Summary of Band Gap Values for WO_3/SnO_2 Thin Films

Material	Bang Gap (eV)
SnO_2	3.82
WO_3/SnO_2 (0.1%)	3.31
WO_3/SnO_2 (0.3%)	3.26
WO_3/SnO_2 (0.5%)	3.05
WO_3/SnO_2 (1.5%)	3.03
WO_3/SnO_2 (2.0%)	3.14

Figure 18

Change in Band gap (E_g) with Doping Proportions of WO_3

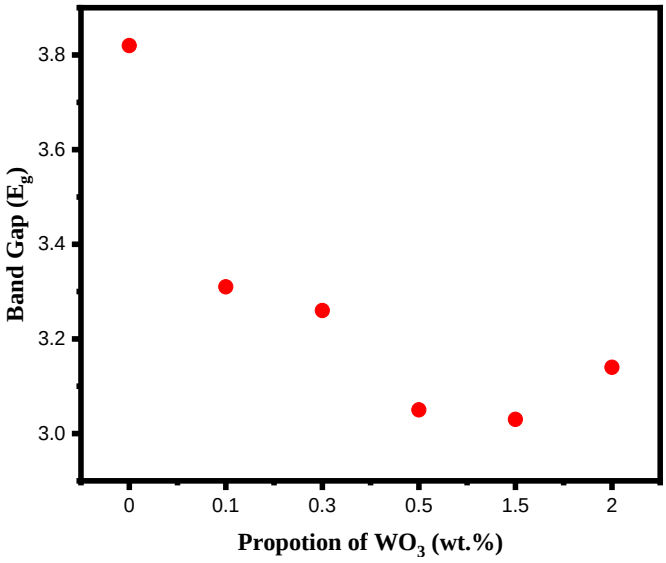

The calculated band gap values are 3.82, 3.31, 3.26, 3.05, 3.03, and 3.14 eVfor SnO_2 and WO_3/SnO_2 (WO_3 of 0.1, 0.5, 1.0, 1.5, 2.0 wt.%) thin films, respectively as shown in table 3. The band gap of undoped $SnO_2$is consistent with work done previously by Bhagwat et al., 2015 and Varghese et al., 2018. As WO_3 was introduced into SnO_2 in various doping proportions, a gradual decrease was observed in the band gap; however, beyond 1.5 %wt. doping, it began to increase as shown in figure 18. This decrease is associated with the red shift observed in the absorbance spectra, which is due to the incorporation of WO_3 into the SnO_2 lattice, which resulted in defects that narrowed the band gap (Ishchenko et al., 2021). This decrease in the band gap is an important factor for the enhancement of photocatalytic activity(Koohestani, 2019). The band gap value for WO_3/SnO_2 (1.5%) is the shortest.

4.2.2.4 Optical Constants (n and k)

4.2.2.4.1. Refractive Index (n)

The refractive index is an important parameter for measuring light absorption during the photocatalytic effect on degradation. A higher refractive index indicates a denser medium (Islam & Kumer, 2020)as a result, the speed of light passing through the material is slower, allowing for more light absorption hence generating more electron-hole pairs that drive photocatalytic reactions. This explains the co-relation of the absorbance profile in figure 15 and the refractive index in figure 19 between 250nm and 450nm. From Figure 19, WO_3doping improves the refractive index of SnO_2. The increase in refractive index with WO_3 doping can be attributed to the films' high porosity (jwad Abdul-Ameer et al., 2018). The photocatalytic activity of a thin semiconducting film is strongly dependent on the film porosity, thickness, and crystallite size, all of which influence the refractive index.

Figure 19

Refractive Index (n) vs wavelength for pure SnO_2 and WO_3/SnO_2 thin films

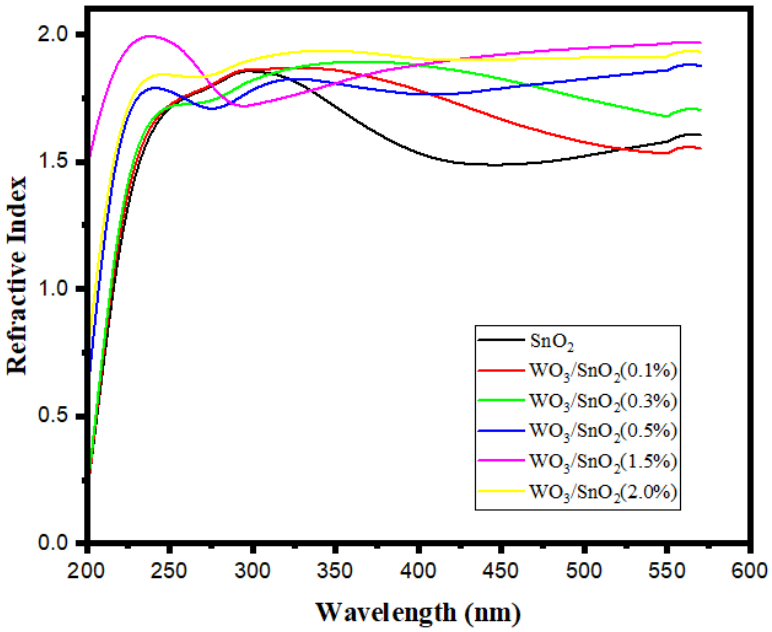

4.2.2.4.2 Extinction Coefficient

Extinction coefficient is a characteristic that determines how strongly a species absorbs or reflects radiation or light at a particular wavelength (Ubi et al., 2022). It is usually used to represent the magnitude of total amount of photons attenuated whenever the electromagnetic waves travel into the target material (Rathanasamy et al., 2023). From Figure 19 below, it is observedthat as wavelength increases, the extinction coefficient decreases. The extinction coefficient, however, increases with dopant concentration and was found to be maximum for the WO_3/SnO_2 (1.5%) sample, resulting in lesser scattering of light (Rathanasamy et al., 2023), and hence the high absorbance observed.

Figure 20

Extinction coefficient (k)as a function of wavelength for pure SnO_2 and WO_3/SnO_2 thin films with different proportions of WO_3

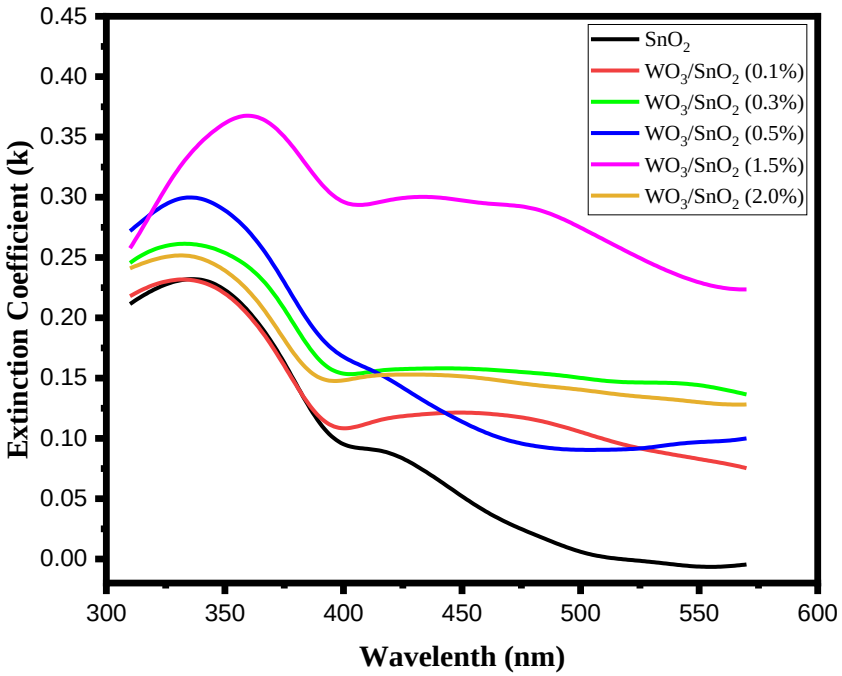

4.2.3 Structural Characterization of the Nanoparticles

The XRD pattern of pure SnO_2 and WO_3/SnO_2 (1.5%) nanoparticles recorded in a 2Θ range from 20^0 to 55^0 is shown in Figure 21 below. The nanoparticles show a number of strong Bragg reflections peaks at different angles, which can be indexed to (110), (101), (200) in the 2Θ range from 20^0 to 55^0 which is consistent with studies done byAkram et al., 2016 and Debataraja et al. 2017.

Figure 21

XRD patterns of (a) SnO_2 (b) WO_3/SnO_2 (1.5%) nanoparticles

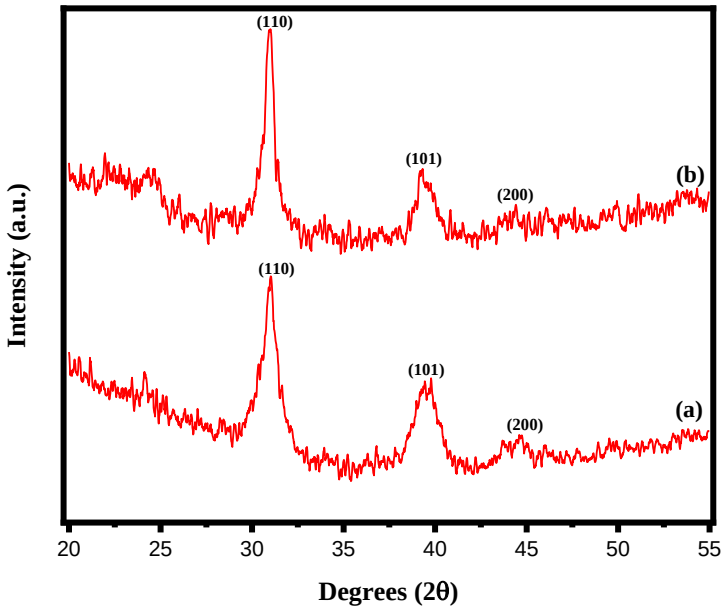

The XRD configuration of both the doped and undoped SnO_2 shown in figure 21 shows that the particles are polycrystalline in structure due to the observed sharp diffraction peaks. From the spectra there was also an indication of some amorphous substance, this is due water present in the structure because of the use of Tin (II) Chloride dihydrate as a precursor which is unstable and is highly hygroscopic hence can easily absorb moisture from the air, which affect the properties of the resulting nanoparticles. The particles preferred orientation along the (110) plane. The (101), and (200) peaks coincide well with standard data (JCPDS Card No.88-0287) (Sagadevan & Podder, 2015).

The crystallite size was determined by Debye-Scherrerś formula given by:

$$D = \frac{0.9\lambda}{\beta cos\theta} \qquad (4.2)$$

Where λ is the wavelength of X-ray radiation (1.7889 Å), and β is the full width half maximum (FWHM) of the peak. The size of the crystallite was determined to be

58.74nm and 89.89nm for SnO_2 and WO_3/SnO_2 (1.5%) as shown in table 4. Larger crystal size has strong correlation to the improvement in photocatalytic performance of materials, (Armaković et al., 2019; Sharma et al., 2014). Therefore the increase in crystal size due to doping SnO_2 is an indication of an improvement in the photocatalytic performance (Nandiyanto et al., 2020).

Table 4

Crystallite Sizes values for pure SnO_2 and WO_3/SnO_2(1.5%)

Material	Crystallite Sizes (nm)
SnO_2	58.74
WO_3/SnO_2 (1.5%)	89.89

4.2.4 Pure SnO_2 andWO_3/SnO_2 Photocatalytic Degradation of Methylene Blue

Based on the optical properties, the WO_3/SnO_2 (1.5%) thin film has superior optical properties for photocatalytic application than all other samples. The photocatalytic properties of pure SnO_2 and WO_3/SnO_2 (1.5%) thin films were investigated using methylene blue dye under UV light. A calibration curve was drawn using standard methylene blue solutions to calculate concentration from measured absorbance, as shown in Figure 22 below.

Figure 22

Methylene Blue Calibration Curve

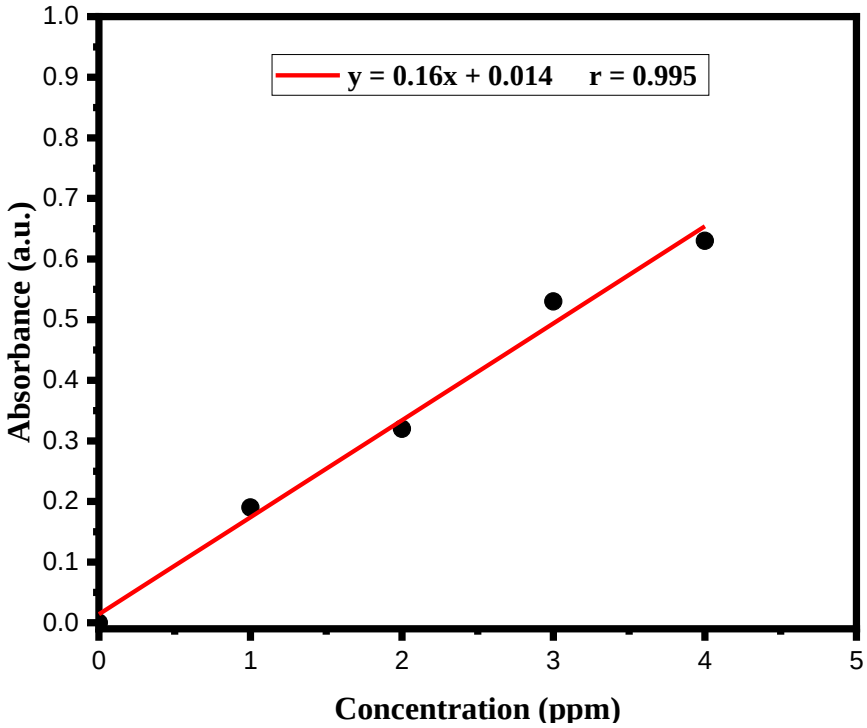

In the photocatalytic experiment, fading of methylene blue solution was seen, showing that degradation was taking place and hence an influence on its concentration. The main absorption peak is located at 664 nm wavelength which corresponds to MB molecules. Figure 23 shows that the absorption peak reduced with increased exposure time, showing that the concentration of dye molecules in the aqueous solution decreased with increasing illumination time.

Figure 23

Absorption Spectra of Methylene Blue for (a) SnO_2 and (b) WO_3/SnO_2 (1.5%) films

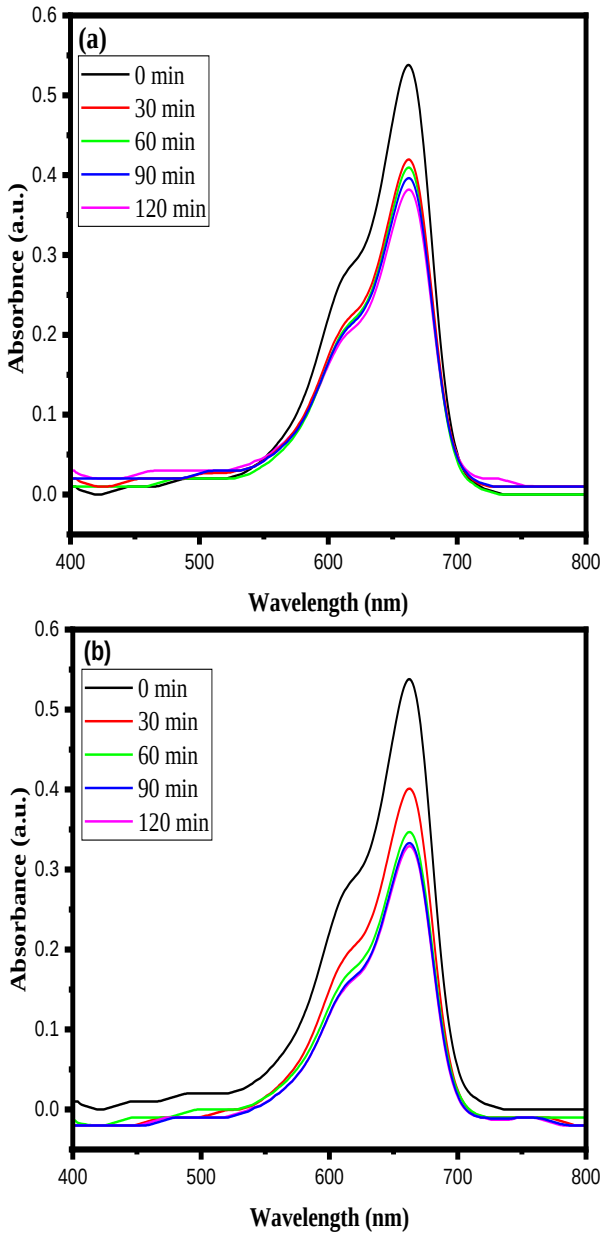

In the photocatalysis mechanism, when light has an energy equal to or more than the band gap is incident on the photocatalyst, this energy is absorbed by the electron in the valence band and gets excited to the conduction band, leaving the holes, thus creating electron–hole pairs. The generated electrons react with the surrounding oxygen and holes react with hydroxide (OH) molecules to form superoxide anions (O^{2-}) and hydroxide

radicals (OH^-), respectively. These O^{2-} and OH^- further react with dye molecules decomposing them into CO_2 and H_2O. The following equations summarize the mechanism;

Activation reaction; $SnO_2 + hv \rightarrow h^+ + e^-$ (4.3)

Oxidation reaction; $h^+ + OH^- \rightarrow OH^{\cdot}$ (4.4)

Reduction reaction; $e^- + O_2 \rightarrow O_2^{\cdot -}$ (4.5)

Organic pollutants + $O_2^{\cdot -}$ (or $OH^{\cdot}$) $\rightarrow CO_2 + H_2O$ (4.6)

The induced photocatalytic degradation of organic pollutants is well known to follow the pseudo first-order kinetic, which exhibits a linear relationship between $ln\ (C_o/C_t)$ and the reaction time. The first-order reaction's kinetics equation is as follows:

$$ln\left(\frac{C_t}{C_o}\right) = -k_c t \quad (4.7)$$

Where; C_t is the Sample concentration after degradation time t, and C_o is the initial Methylene Blue concentation. Figure 24 shows a graph of $ln\ (C_o/C_t)$ versus time in minutes for sampled films of the pure SnO_2 and WO_3/SnO_2 (1.5 w.t%) thin films.

Figure 24

Plots of (a) $ln\ (C_o/C)$ vs Irradiation time

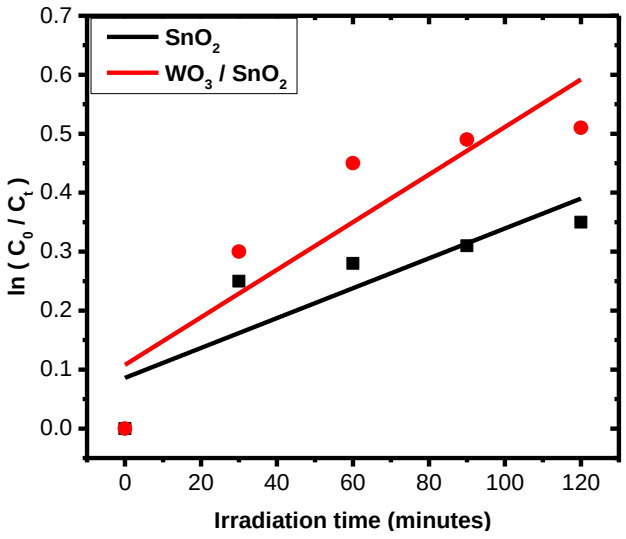

The gradient of the plot in figure 24 was used to find the rate constant, k_c (indicated in figure 25) this enabled evaluation of the photocatalytic activity of the synthesized samples. The rate constant dictates how quickly degradation occurs. The calculated rate constant values from the above relation are 0.00256 and 0.00519 min^{-1} for SnO_2 and WO_3/SnO_2 (1.5%) films, respectively.

Figure 25

Influence of WO_3 doping on the Reaction Rate Constant

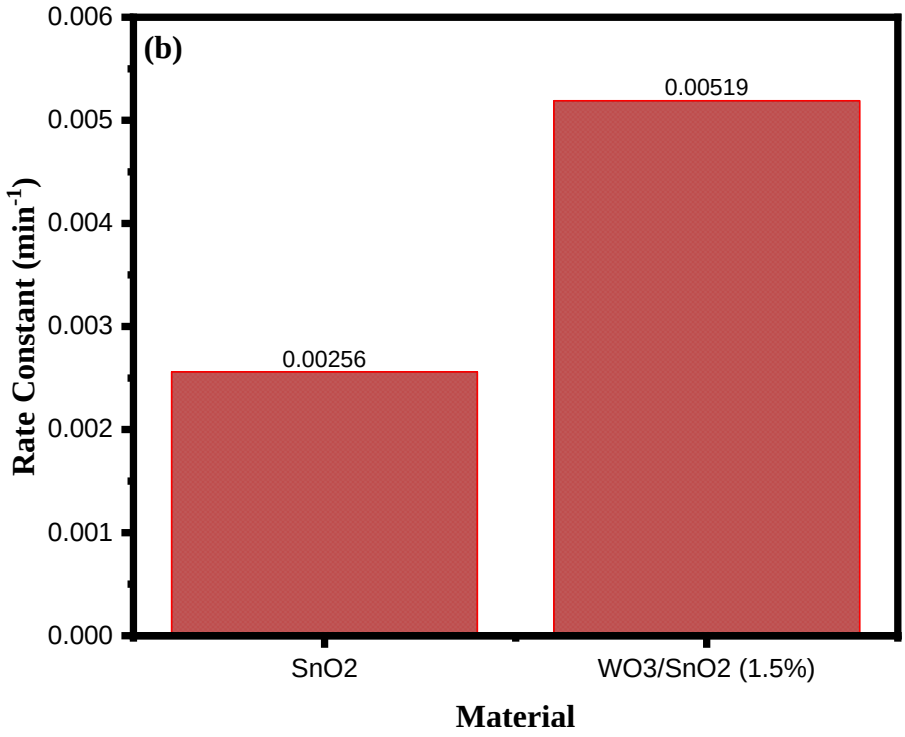

Based on the obtained the results, WO_3/SnO_2 is more efficient than pure SnO_2, this can be attributed to the following:

(i) Decreased SnO_2 band gap after WO_3 incorporation, from 3.82 to 3.03 eV. This decrease is important in increasing photocatalytic activity (Koohestani, 2019) because more electrons are able to gain kinetic energy and move to the conduction band, where they participate in the degradation process.

(ii) Decreased electron-hole pair (EHP) recombination as a result of WO_3 incorporation into the SnO_2 lattice; WO_3 acts as a trap to easily capture the photogenerated electrons and holes on the surface of SnO_2 and thus delay EHP recombination (Manikandan et al., 2018), which would otherwise decrease the photocatalytic activity of SnO_2.

(iii) Improved light absorption of WO_3/SnO_2 indicating that more radiation is absorbed exciting more electrons to the conduction band participating in the degradation process(Enesca & Sisman, 2022).

(iv) Increased crystallite size of WO_3/SnO_2 from 58.74 to 89.89nm. A larger crystal size has strong correlation to the improvement in photocatalytic performance of materials(Nandiyanto et al., 2020), which is in agreement with similar studies bySharma et al., 2014 andArmaković et al., 2019.

These findings of this research are in agreement with that of Ramos-Delgado et al., 2013, who found that WO_3/TiO_2 showed improved photocatalytic behavior than bare TiO_2 due to the formation of smaller clusters and a larger surface area that decreases electron-hole pair recombination and results in a better contact area between the catalyst particles and the pollutant, improving photocatalytic reactivity (Ramos-Delgado et al., 2013)

CHAPTER FIVE

SUMMARY, CONCLUSION AND RECOMMENDATIONS

5.1. Introduction

This chapter offers a summary of the findings of this study, conclusions, and recommendations for further research.

5.2. Summary

Pure SnO_2 and WO_3/SnO_2 were successfully prepared through the Sol-gel spin coating technique. The influence of the WO_3 doping over the optical, structural and photocatalytic properties of $SnO_2$was investigated. A UV-VIS 2600 spectrophotometer was employed for optical characterization of the fabricated films and absorbance measurements were obtained whichshowed that WO_3/SnO_2 thin films have enhanced absorbance with the peak absorbance shifting towards longer wavelengths. Optical analysis shows that the deposited WO_3/SnO_2thin films have a decreased band gap from 3.82 to 3.03 eV, confirming that these are good semiconducting films. An X-ray diffraction equipment Olympus TERRA-538(Fisonga et al., 2022) was employed for structural characterization which showed that the samples are crystalline. The photocatalytic activity of the prepared films was investigated with Methylene Blue dye under UV irradiation.WO_3/SnO_2films show superior photocatalytic activity than the undoped SnO_2 films. Therefore,doping $SnO_2$with $WO_3$is very effective in improving its photocatalytic properties. These results show that low-cost WO_3/SnO_2 photocatalyst is a good candidate to eliminate organic pollutants from contaminated water, which cause severe threats to health and the environment.

5.3. Conclusion

5.3.1. Fabrication of SnO_2 and WO_3/SnO_2 Thin Films

SnO_2 and WO_3/SnO_2 thin films were successfully prepared through the Sol-gel Spin coating technique at a rotary speed of 1200 Rpm for 30 sec. This method was employed because it is one of the simplest, quickest, and low cost techniques, with several advantages such as controlled stoichiometry, better homogeneity, low processing temperature, high purity, effective control of properties such as film thickness, and the capacity to easily scale up.

The average film thickness of the fabricated films was modelled using SCOUT software where the obtained experimental spectra was fitted to the simulated spectra within the software with a suitable optical model. This was used since the necessary equipment that would have been used to measure the film thickness directly such as Alpha step or Atomic Force Microscope (AFM) was not working.

5.3.2. Determination of Optical and Structural Properties of Pure SnO_2 and WO_3/SnO_2

The effect of the WO_3 doping over the optical properties & structural properties of the prepared SnO_2 and WO_3/SnO_2 have been investigated. The properties obtained in optical characterization are absorbance, refractive index, extinction coefficient and the band gap energy of the fabricated films. The SnO_2 doped films were found to generally have a high absorbance; the absorbance increased with increase in the dopant proportion. However, doping beyond 1.5 w.t% instead decreased the absorbance. Doping resulted to a red shift of the absorption edge with the peak absorbance shifting towards longer

wavelengths, indicating a decrease in band gap.

Further Optical analysis show that the deposited WO_3/SnO_2 thin films have a reduced band gap energy from 3.82 to 3.03 eV confirming that these are good semiconducting films. The decrease in band gap confirmed the red shift noticed in the absorption edge.

Structural Characterization shows that the prepared samples are crystalline. Doped SnO_2 crystallite size was found to be large compared to pure SnO_2 showing that there has been an improvement in the structural properties of SnO_2 due to incorporation of WO_3 for photocatalytic dye degradation.

5.3.3. Photocatalytic Performance of Pure SnO_2 and SnO_2 Doped with WO_3

The photocatalytic activity of the deposited films has been studied against Methylene Blue dye under UV irradiation. WO_3/SnO_2 films show superior photocatalytic activity than undoped SnO_2 film. Therefore, SnO_2 doping with WO_3 is very effective for improving SnO_2 photocatalytic properties. As a result, the WO_3/SnO_2 catalyst is a good candidate for the removal of toxic organic pollutants from contaminated water.

5.4. Recommendation for Further Research

i) The results obtained and described in this study demonstrate a strong effect of WO_3 on the optical, structural, and photocatalytic characteristics of SnO_2. This study, however, was limited to optical and structural aspects exclusively. Other elements influencing photocatalysis include chemical characteristics and surface

morphology. It is therefore suggested that surface and chemical characterization of the films be done, to evaluate the effect of doping on the surface morphology, chemical structure, and orientation of synthesized samples. This can be studied using Scanning Electron Microscopy (SEM), Transmission Electron Microscopy (TEM), Raman spectroscopy, and X-ray photoelectron spectroscopy (XPS).

ii) Previous studies have indicated that the solvent used to prepare Tin (IV) Oxide thin films has a significant influence on some of its optical and structural properties, which are also very critical for photocatalytic applications. Therefore, future work can be done using different solvents such as Methanol and Isopropanol to see how they influence the photocatalytic efficiency of the prepared material.

iii) Further study is required to characterize the electrical properties and investigate additional deposition factors to improve the films for optoelectronic device applications. Furthermore, the influence of varying annealing temperatures and film thicknesses requires to be explored to improve film characteristics for specific applications.

iv) Further investigation to be done to determine Influence of film thickness on the photocatalytic activity of the WO_3/SnO_2 thin films by varying the spin speed and spin time of the spin coater. This will establish the optimum film thickness of the films since it has been established that film thickness also influences the photocatalytic activity of the films.

v) Surfactants have previously been studied and reported to influence the structural morphology, physicochemical properties and contaminant removal performance of photocatalysts. Therefore future studies can be done to prepare surfactant-assisted photocatalyst of WO_3/SnO_2 to establish its influence.

REFFERENCES

Abd-Elnaiem, A. M., & Hakamy, A. (2022). Influence of annealing temperature on structural, electrical, and optical properties of 80 nm thick indium-doped tin oxide on borofloat glass. *Journal of Materials Science: Materials in Electronics*, *33*(30), 23293–23305.

Abdullah, A. M., Al-Thani, N. J., Tawbi, K., & Al-Kandari, H. (2016). Carbon/nitrogen-doped TiO2: New synthesis route, characterization and application for phenol degradation. *Arabian Journal of Chemistry*, *9*(2), 229–237.

Aghgonbad, M. M., & Sedghi, H. (2018). Influence of annealing temperature on optical properties of zinc oxide thin films analyzed by spectroscopic ellipsometry method. *Chinese Journal of Physics*, *56*(5), 2129–2138.

Akram, M., Saleh, A., Wan Ibrahim, W. A., Awan, A., & Hussain, R. (2016). Continuous microwave flow synthesis (CMFS) of nano-sized tin oxide: Effect of precursor concentration. *Ceramics International*, *42*. https://doi.org/1 0.1016/j.cera mint.2016.02.092

Al-Hamdi, A. M., Rinner, U., & Sillanpää, M. (2017). Tin dioxide as a photocatalyst for water treatment: a review. *Process Safety and Environmental Protection*, *107*, 190–205.

Ali, T., Tripathi, P., Azam, A., Raza, W., Ahmed, A. S., Ahmed, A., & Muneer, M. (2017). Photocatalytic performance of Fe-doped TiO2 nanoparticles under visible-light irradiation. *Materials Research Express*, *4*(1). https://doi.org/10.1 088/2053-1591/aa576d

Alshammari, A., Bagabas, A., & Assulami, M. (2019). Photodegradation of rhodamine B over semiconductor supported gold nanoparticles: the effect of semiconductor support identity. *Arabian Journal of Chemistry*, *12*(7), 1406–1412.

Anandan, K., & Rajendran, V. (2015). Influence of dopant concentrations (Mn= 1, 2 and 3 mol%) on the structural, magnetic and optical properties and photocatalytic activities of SnO2 nanoparticles synthesized via the simple precipitation process. *Superlattices and Microstructures*, *85*, 185–197.

Arai, T., Yanagida, M., Konishi, Y., Iwasaki, Y., Sugihara, H., & Sayama, K. (2008). Promotion effect of CuO co-catalyst on WO3-catalyzed photodegradation of organic substances. *Catalysis Communications*, *9*(6), 1254–1258.

Armaković, S. J., Grujić-Brojčin, M., Šćepanović, M., Armaković, S., Golubović, A., Babić, B., & Abramović, B. F. (2019). Efficiency of La-doped TiO2 calcined at different temperatures in photocatalytic degradation of β-blockers. *Arabian Journal of Chemistry*, *12*(8), 5355–5369.

Arutanti, O., Ogi, T., Nandiyanto, A. B. D., Iskandar, F., & Okuyama, K. (2014). Controllable crystallite and particle sizes of WO3 particles prepared by a spray- pyrolysis method and their photocatalytic activity. *AIChE Journal*, *60*(1), 41–49.

Azim, M. B., Jani, M., Qadir, M., Hasanuzzaman, M., Gafur, M., Gulshan, F., & Firoz, S. (2021). *GO-SnO2 Nanocomposite for Photodegradation of Methyl Orange Under Direct Sunlight Irradiation and Mechanism Insight*.

Badli, N. A., Ali, R., Bakar, W. A. W. A., & Yuliati, L. (2017). Role of heterojunction ZrTiO4/ZrTi2O6/TiO2 photocatalyst towards the degradation of paraquat dichloride and optimization study by Box–Behnken design. *Arabian Journal of Chemistry*, *10*(7), 935–943.

Behnajady, M. A., Modirshahla, N., & Hamzavi, R. (2006). Kinetic study on photocatalytic degradation of CI Acid Yellow 23 by ZnO photocatalyst. *Journal of Hazardous Materials*, *133*(1–3), 226–232.

Bhagwat, A. D., Sawant, S. S., Ankamwar, B. G., & Mahajan, C. M. (2015). *Synthesis of nanostructured tin oxide (SnO2) powders and thin films prepared by sol-gel method*.

Bhattacharjee, A., & Ahmaruzzaman, M. (2015). Photocatalytic-degradation and reduction of organic compounds using SnO 2 quantum dots (via a green route) under direct sunlight. *RSC Advances*, *5*(81), 66122–66133.

Boshta, M., Mahmoud, F. A., & Sayed, M. H. (2010). Characterization of sprayed SnO2: Pd thin films for gas sensing applications. *Journal of Ovonic Research*, *6*(2), 93–98.

Boudrioua, A., Chakaroun, M., & Fischer, A. (2017). Organic light-emitting diodes. *Organic Lasers*, 49–93.

Bouras, K., Rehspringer, J.-L., Schmerber, G., Rinnert, H., Colis, S., Ferblantier, G., Balestrieri, M., Ihiawakrim, D., Dinia, A., & Slaoui, A. (2014). Optical and structural properties of Nd doped SnO 2 powder fabricated by the sol–gel method. *Journal of Materials Chemistry C*, *2*(39), 8235–8243.

Britannica, E. (2022). *Fujishima. Akira | Japanese chemist*. Www.Britannica.Com. https://www.britannica.com/biography/Fujishima-Akira

Buchholz, K. (2022). *Unsafe Water Kills More People Than Disasters and Conflicts*. Statista.https://www.statista.com/chart/17445/global-access-to-safe-drinking-water/

Chatterjee, D., & Dasgupta, S. (2005). Visible light induced photocatalytic degradation of organic pollutants. *Journal of Photochemistry and Photobiology C: Photochemistry Reviews*, *6*(2–3), 186–205.

Chaudhary, K. T. (2021). Thin film deposition: Solution based approach. In *Thin Films*. IntechOpen.

Chebwogen, J. (2019). *Fabrication and characterization of cobalt pigmented anodized zinc for photocatalytic application*. KABARAK UNIVERSITY.

Chebwogen, J., Maghanga, C., Mwamburi, M., Munyati, O., Hatwaambo, S., & Kebenei, S. (2019). *Optical Characterization Of Co: Zno Films Fabricated By Anodization For Photocatalytic Water Purification*.

Chen, P., Liu, H., Cui, W., Lee, S. C., Wang, L., & Dong, F. (2020). Bi- based photocatalysts for light- driven environmental and energy applications: Structural tuning, reaction mechanisms, and challenges . *EcoMat*, *2*(3), 1–31. https://doi.org/10.1002/eom2.12047

Cheng, H., Huang, B., Lu, J., Wang, Z., Xu, B., Qin, X., Zhang, X., & Dai, Y. (2010). Synergistic effect of crystal and electronic structures on the visible-light-driven photocatalytic performances of Bi 2 O 3 polymorphs. *Physical Chemistry Chemical Physics*, *12*(47), 15468–15475.

Choi, D., & Park, J.-S. (2014). Highly conductive SnO2 thin films deposited by atomic layer deposition using tetrakis-dimethyl-amine-tin precursor and ozone reactant. *Surface and Coatings Technology*, *259*, 238–243.

Churbanov, M. F., Moiseev, A. N., Chilyasov, A. V, Dorofeev, V. V, Kraev, I. A., Lipatova, M. M., Kotereva, T. V, Dianov, E. M., Plotnichenko, V. G., & Kryukova, E. B. (2007). Production of high-purity TeO2-ZnO and TeO2-WO3 glasses with the reduced content of OH-groups. *J. Optoelectron. Adv. M.*, *9*(10), 3229–3234.

Crini, G., & Lichtfouse, E. (2019). Advantages and disadvantages of techniques used for wastewater treatment. *Environmental Chemistry Letters*, *17*, 145–155.

Danks, A. E., Hall, S. R., & Schnepp, Z. (2016). The evolution of 'sol–gel'chemistry as a technique for materials synthesis. *Materials Horizons*, *3*(2), 91–112.

De Wijs, G. A., & De Groot, R. A. (1999). Structure and electronic properties of amorphous WO 3. *Physical Review B*, *60*(24), 16463.

Debataraja, A., Zulhendri, D. W., Yuliarto, B., & Sunendar, B. (2017). Investigation of nanostructured SnO2 synthesized with polyol technique for CO gas sensor applications. *Procedia Engineering*, *170*, 60–64.

Doyan, A., Hakim, S., Muliyadi, L., & Taufik, M. (2019). The Effect of Indium Doped SnO2 Thin Films on Optical Properties Prepared by Sol-Gel Spin Coating Technique. *Journal of Physics: Conference Series*, *1397*(1), 12005.

Educator, P. (2022). *Absorption Coefficient*. Pveducation.Org. https://www.pveducation .org/pvcdrom/pn-j unctions/absorption-coefficient

Enesca, A., & Sisman, V. (2022). Indoor Air Photocatalytic Decontamination by UV–Vis Activated CuS/SnO2/WO3 Heterostructure. *Catalysts*, *12*(7), 728.

Fisonga, M., Korir, E., Chipola, P., & Mutambo, V. (2022). Geotechnical Characterization of Alisol Soils in Eastern Province of Zambia. *Journal of Natural and Applied Sciences*, *6*(1), 14–31.

Gajbhiye, S. B. (2012). Photocatalytic degradation study of methylene blue solutions and its application to dye industry effluent. *Int. J. Mod. Eng. Res*, *2*(3), 1204–1208.

Gao, M., Zhu, L., Peh, C. K., & Ho, G. W. (2019). Solar absorber material and system designs for photothermal water vaporization towards clean water and energy production. *Energy & Environmental Science*, *12*(3), 841–864.

HA Jalaukhan, A., Ghanbari Shohany, B., & Etefagh, R. (2021). Preparation and investigation of optical properties and photocatalytic activity of SnO2/GO thin films. *Scientia Iranica*, *28*(3), 1908–1916.

Han, W., Ren, L., Qi, X., Liu, Y., Wei, X., Huang, Z., & Zhong, J. (2014). Synthesis of CdS/ZnO/graphene composite with high-efficiency photoelectrochemical activities under solar radiation. *Applied Surface Science*, *299*, 12–18.

Haouanoh, D., TalaIghil, R. Z., Toubane, M., Bensouici, F., & Mokeddem, K. (2019). Effects of thermal treatment and layers' number on SnO2 thin films properties prepared by sol-gel technique. *Materials Research Express*, *6*(8), 86422.

Hariganesh, S., Vadivel, S., Maruthamani, D., & Rangabhashiyam, S. (2020). Disinfection by-products in drinking water: detection and treatment methods. In *Disinfection By-products in Drinking Water* (pp. 279–304). Elsevier.

Hasija, V., Sudhaik, A., Raizada, P., Hosseini-Bandegharaei, A., & Singh, P. (2019). Carbon quantum dots supported AgI/ZnO/phosphorus doped graphitic carbon nitride as Z-scheme photocatalyst for efficient photodegradation of 2, 4-dinitrophenol. *Journal of Environmental Chemical Engineering*, *7*(4), 103272.

Hayashi, H., Ishizaka, A., Haemori, M., & Koinuma, H. (2003). Bright blue phosphors in ZnO–WO 3 binary system discovered through combinatorial methodology. *Applied Physics Letters*, *82*(9), 1365–1367.

Holden, T., Ram, P., Pollak, F. H., Freeouf, J. L., Yang, B. X., & Tamargo, M. C. (1997). Spectral ellipsometry investigation of Zn 0.53 Cd 0.47 Se lattice matched to InP. *Physical Review B*, *56*(7), 4037.

Hsu, C.-H., Geng, X.-P., Wu, W.-Y., Zhao, M.-J., Zhang, X.-Y., Huang, P.-H., & Lien, S.-Y. (2020). Air annealing effect on oxygen vacancy defects in Al-doped ZnO films grown by high-speed atmospheric atomic layer deposition. *Molecules*, *25*(21), 5043.

Huang, T., Qiu, Z., Hu, Z., & Lu, X. (2021). Novel method of preparing hierarchical porous CoFe2O4 by the citric acid-assisted sol-gel auto-combustion for supercapacitors. *Journal of Energy Storage*, *35*, 102286.

Iqbal, T., Khan, M. A., & Mahmood, H. (2018). Facile synthesis of ZnO nanosheets: Structural, antibacterial and photocatalytic studies. *Materials Letters*, *224*, 59–63.

Ishchenko, O., Rogé, V., Lamblin, G., Lenoble, D., & Fechete, I. (2021). TiO $ _ {2} $, ZnO, and SnO $ _ {2} $-based metal oxides for photocatalytic applications: principles and development. *Comptes Rendus. Chimie*, *24*(1), 103–124.

Islam, M. J., & Kumer, A. (2020). First-principles study of structural, electronic and optical properties of AgSbO3 and AgSb0. 78Se0. 22O3 photocatalyst. *SN Applied Sciences*, *2*(2), 251.

Jilani, A., Abdel-wahab, M. S., & Hammad, A. H. (2017). Advance Deposition Techniques for Thin Film and Coating. *Modern Technologies for Creating the Thin-Film Systems and Coatings*. https://doi.org/10.5772/65702

jwad Abdul-Ameer, H., Al-Hilli, M. F., & Khalaf, M. K. (2018). Comparative NO2 Sensing Characteristics of SnO2: WO3 Thin Film Against Bulk and Investigation of Optical Properties of the Thin Film. *Baghdad Science Journal*, *15*(2).

Karouei, S. F. H., & Moghaddam, H. M. (2019). Pp heterojunction of polymer/hierarchical mesoporous LaFeO3 microsphere as CO2 gas sensing under high humidity. *Applied Surface Science*, *479*, 1029–1038.

Katwal, R., Kothari, R., & Pathania, D. (2021). An overview on degradation kinetics of organic dyes by photocatalysis using nanostructured electrocatalyst. *Delivering Low-Carbon Biofuels with Bioproduct Recovery*, 195–213.

Kianfar, E., & Suksatan, W. (2021). Nanomaterial by Sol-Gel Method: Synthesis and Application. *Advances in Materials Science and Engineering*, *2021*, 1–21. https://doi.org/10.1155/2021/5102014

Kočí, K., Matějová, L., Ambrožová, N., Šihor, M., Troppová, I., Čapek, L., Kotarba, A., Kustrowski, P., Hospodková, A., & Obalová, L. (2016). Optimization of cerium doping of TiO 2 for photocatalytic reduction of CO 2 and photocatalytic decomposition of N 2 O. *Journal of Sol-Gel Science and Technology*, *78*, 550–558.

Koe, W. S., Lee, J. W., Chong, W. C., Pang, Y. L., & Sim, L. C. (2020). An overview of photocatalytic degradation: photocatalysts, mechanisms, and development of photocatalytic membrane. *Environmental Science and Pollution Research*, *27*, 2522–2565.

Koohestani, H. (2019). Characterization of TiO2/WO3 composite produced with recycled WO3 nanoparticles from WNiFe alloy. *Materials Chemistry and Physics*, *229*, 251–256.

Lee, S. H., Hoffman, D. M., Jacobson, A. J., & Lee, T. R. (2013). Transparent, homogeneous tin oxide (SnO2) thin films containing SnO2-coated gold nanoparticles. *Chemistry of Materials*, *25*(23), 4697–4702.

Legutko, P., Stelmachowski, P., Trębala, M., Sojka, Z., & Kotarba, A. (2013). Role of electronic factor in soot oxidation process over tunnelled and layered potassium iron oxide catalysts. *Topics in Catalysis*, *56*, 489–492.

Liu, B., & Aydil, E. S. (2009). Growth of oriented single-crystalline rutile TiO2 nanorods on transparent conducting substrates for dye-sensitized solar cells. *Journal of the American Chemical Society*, *131*(11), 3985–3990.

Liu, J., Wang, C., Yang, Q., Gao, Y., Zhou, X., Liang, X., Sun, P., & Lu, G. (2016). Hydrothermal synthesis and gas-sensing properties of flower-like Sn3O4. *Sensors and Actuators B: Chemical*, *224*, 128–133.

Mahdi, M. A., Yousefi, S. R., Jasim, L. S., & Salavati-Niasari, M. (2022). Green synthesis of DyBa2Fe3O7. 988/DyFeO3 nanocomposites using almond extract with dual eco-friendly applications: photocatalytic and antibacterial activities. *International Journal of Hydrogen Energy*, *47*(31), 14319–14330.

Maniak, G., Stelmachowski, P., Stanek, J. J., Kotarba, A., & Sojka, Z. (2011). Catalytic properties in N2O decomposition of mixed cobalt–iron spinels. *Catalysis Communications*, *15*(1), 127–131.

Manikandan, A. S., Renukadevi, K. B., Ravichandran, K., & Sindhuja, E. (2018). Ag activated SnO 2 films for enhanced photocatalytic dye degradation against toxic organic dyes. *Journal of Materials Science: Materials in Electronics*, *29*, 8547–8554.

Marikkannan, M., Vishnukanthan, V., Vijayshankar, A., Mayandi, J., & Pearce, J. M. (2015). A novel synthesis of tin oxide thin films by the sol-gel process for optoelectronic applications. *Aip Advances*, *5*(2), 27122.

Marotti, R. E., Giorgi, P., Machado, G., & Dalchiele, E. A. (2006). Crystallite size dependence of band gap energy for electrodeposited ZnO grown at different temperatures. *Solar Energy Materials and Solar Cells*, *90*(15), 2356–2361.

Matějová, L., Kočí, K., Reli, M., Čapek, L., Hospodková, A., Peikertová, P., Matěj, Z., Obalová, L., Wach, A., & Kuśtrowski, P. (2014). Preparation, characterization and photocatalytic properties of cerium doped TiO2: On the effect of Ce loading on the photocatalytic reduction of carbon dioxide. *Applied Catalysis B: Environmental*, *152*, 172–183.

Matějová, L., Šihor, M., Brunátová, T., Ambrožová, N., Reli, M., Čapek, L., Obalová, L., & Kočí, K. (2015). Microstructure-performance study of cerium-doped TiO 2 prepared by using pressurized fluids in photocatalytic mitigation of N 2 O. *Research on Chemical Intermediates*, *41*, 9217–9231.

McNaught, A. D. (1997). *A. Wilkinson in IUPAC Gold Book-Compendium of Chemical Terminology*. Blackwell Scientific Publications, Oxford.

Minami, T., & Miyata, T. (2008). Present status and future prospects for development of non-or reduced-indium transparent conducting oxide thin films. *Thin Solid Films*, *517*(4), 1474–1477.

Molinari, R., Lavorato, C., & Argurio, P. (2020). Visible-light Photocatalysts and their perspectives various liquid phase chemical conversions. *Catalysts I*, 1–38.

Moma, J., & Baloyi, J. (2019). Modified titanium dioxide for photocatalytic applications. *Photocatalysts-Applications and Attributes*, *18*, 10–5772.

Mouhamad, Y., Mokarian-Tabari, P., Clarke, N., Jones, R. A. L., & Geoghegan, M. (2014). Dynamics of polymer film formation during spin coating. *Journal of Applied Physics*, *116*(12), 123513.

Nabi, Z., Kellou, A., Mecabih, S., Khalfi, A., & Benosman, N. (2003). Opto-electronic properties of rutile SnO2 and orthorhombic SnS and SnSe compounds. *Materials Science and Engineering: B*, *98*(2), 104–115.

Nadarajan, R., Bakar, W. A. W. A., Ali, R., & Ismail, R. (2018). Photocatalytic degradation of 1, 2-dichlorobenzene using immobilized TiO2/SnO2/WO3 photocatalyst under visible light: Application of response surface methodology. *Arabian Journal of Chemistry*, *11*(1), 34–47.

Nagaveni, K., Hegde, M. S., Ravishankar, N., Subbanna, G. N., & Madras, G. (2004). Synthesis and structure of nanocrystalline TiO2 with lower band gap showing high photocatalytic activity. *Langmuir*, *20*(7), 2900–2907.

Nandiyanto, A. B. D., Arutanti, O., Ogi, T., Iskandar, F., Kim, T. O., & Okuyama, K. (2013). Synthesis of spherical macroporous WO3 particles and their high photocatalytic performance. *Chemical Engineering Science*, *101*, 523–532.

Nandiyanto, A. B. D., Iskandar, F., & Okuyama, K. (2009). Macroporous anatase titania particle: Aerosol self-assembly fabrication with photocatalytic performance. *Chemical Engineering Journal*, *152*(1), 293–296.

Nandiyanto, A. B. D., Sofiani, D., Permatasari, N., Sucahya, T. N., Wiryani, A. S., Purnamasari, A., Rusli, A., & Prima, E. C. (2016). Photodecomposition profile of organic material during the partial solar eclipse of 9 march 2016 and its correlation with organic material concentration and photocatalyst amount. *Indonesian Journal of Science and Technology*, *1*(2), 132–155.

Nandiyanto, A. B. D., Wiryani, A. S., Rusli, A., Purnamasari, A., Abdullah, A. G., Widiaty, I., & Hurriyati, R. (2017). Extraction of curcumin pigment from Indonesian local turmeric with its infrared spectra and thermal decomposition properties. *IOP Conference Series: Materials Science and Engineering*, *180*(1), 12136.

Nandiyanto, A. B. D., Zaen, R., & Oktiani, R. (2020). Correlation between crystallite size and photocatalytic performance of micrometer-sized monoclinic WO3 particles. *Arabian Journal of Chemistry*, *13*(1), 1283–1296.

Naseri, N., Azimirad, R., Akhavan, O., & Moshfegh, A. Z. (2010). Improved electrochromical properties of sol–gel WO3 thin films by doping gold nanocrystals. *Thin Solid Films*, *518*(8), 2250–2257.

Obalová, L., Maniak, G., Karásková, K., Kovanda, F., & Kotarba, A. (2011). Electronic nature of potassium promotion effect in Co–Mn–Al mixed oxide on the catalytic decomposition of N2O. *Catalysis Communications*, *12*(12), 1055–1058.

Ojha, A., & Tiwary, D. (2021). Organic pollutants in water and its health risk assessment through consumption. In *Contamination of Water* (pp. 237–250). Elsevier.

Pankove, J. I. (1975). *Optical processes in semiconductors*. Courier Corporation.

Paras, & Kumar, A. (2021). *Anti-Wetting Polymeric Coatings*.

Parashar, M., Shukla, V. K., & Singh, R. (2020). Metal oxides nanoparticles via sol–gel method: a review on synthesis, characterization and applications. *Journal of Materials Science: Materials in Electronics*, *31*, 3729–3749.

Pascariu, P., Tudose, I. V., & Suchea, M. (2019). Surface morphology effects on photocatalytic activity of metal oxides nanostructured materials immobilized onto substrates. *Journal of Nanoscience and Nanotechnology*, *19*(1), 295–306.

Patel, G. H., Chaki, S. H., Kannaujiya, R. M., Parekh, Z. R., Hirpara, A. B., Khimani, A. J., & Deshpande, M. P. (2021). Sol-gel synthesis and thermal characterization of SnO2 nanoparticles. *Physica B: Condensed Matter*, *613*, 412987.

Patterson, J., & Bailey, B. (2010). Solid-state physics: Introduction to the theory. In *Solid-State Physics (Second Edition): Introduction to the Theory*. https://doi.org/10.1007/978-3-642-02589-1

Peiró, A. M., Peral, J., Domingo, C., Domènech, X., & Ayllón, J. A. (2001). Low-temperature deposition of TiO2 thin films with photocatalytic activity from colloidal anatase aqueous solutions. *Chemistry of Materials*, *13*(8), 2567–2573.

Piaskowski, K., Świderska-Dąbrowska, R., & Zarzycki, P. K. (2018). Dye removal from water and wastewater using various physical, chemical, and biological processes. *Journal of AOAC International*, *101*(5), 1371–1384.

Pierre, A. C. (2020). *Introduction to sol-gel processing*. Springer Nature.

Praveen, P. L., & Ojha, D. P. (2014). Effect of substituent on UV–visible absorption and photostability of liquid crystals: DFT study. *Phase Transitions*, *87*(5), 515–525.

Radhika, N. P., Selvin, R., Kakkar, R., & Umar, A. (2019). Recent advances in nano-photocatalysts for organic synthesis. *Arabian Journal of Chemistry*, *12*(8), 4550–4578.

Raj, I. L. P., Revathy, M. S., Christy, A. J., Chidhambaram, N., Ganesh, V., & AlFaify, S. (2020). Study on the synergistic effect of terbium-doped SnO 2 thin film photocatalysts for dye degradation. *Journal of Nanoparticle Research*, *22*, 1–14.

Ramírez-Santos, Á. A., Acevedo-Peña, P., & Córdoba, E. M. (2012). Enhanced photocatalytic activity of TiO2 films by modification with polyethylene glycol. *Quimica Nova*, *35*, 1931–1935.

Ramos-Delgado, N. A., Gracia-Pinilla, M. A., Maya-Trevino, L., Hinojosa-Reyes, L., Guzman-Mar, J. L., & Hernández-Ramírez, A. (2013). Solar photocatalytic activity of TiO2 modified with WO3 on the degradation of an organophosphorus pesticide. *Journal of Hazardous Materials*, *263*, 36–44.

Rathanasamy, R., Kaliyannan, G. V., Sivaraj, S., Muthiah, E., Khaan, A. A. A., Ravichandran, D., & Uddin, M. (2023). Effect of Molybdenum Disulphide Thin Films on Enhancing the Performance of Polycrystalline Silicon Solar Cells. *International Journal of Photoenergy*, *2023*.

Rathod, J. R. (2014). *Investigations on the growth and characterization of znte thin films deposited by Silar method for possible window applications*.

Reli, M., Ambrožová, N., Šihor, M., Matějová, L., Čapek, L., Obalová, L., Matěj, Z., Kotarba, A., & Kočí, K. (2015). Novel cerium doped titania catalysts for photocatalytic decomposition of ammonia. *Applied Catalysis B: Environmental*, *178*, 108–116.

Sagadevan, S., & Podder, J. (2015). *Optical and electrical properties of nanocrystalline SnO2 thin films synthesized by chemical bath deposition method*.

Sakthivel, S., Neppolian, B., Shankar, M. V, Arabindoo, B., Palanichamy, M., & Murugesan, V. (2003). Solar photocatalytic degradation of azo dye: comparison of photocatalytic efficiency of ZnO and TiO2. *Solar Energy Materials and Solar Cells*, *77*(1), 65–82.

Sap, J. A., Isabella, O., Jäger, K., & Zeman, M. (2011). Extraction of optical properties of flat and surface-textured transparent conductive oxide films in a broad wavelength range. *Thin Solid Films*, *520*(3), 1096–1101.

Sefardjella, H., Boudjema, B., Kabir, A., & Schmerber, G. (2013). Characterization of SnO2 obtained from the thermal oxidation of vacuum evaporated Sn thin films. *Journal of Physics and Chemistry of Solids*, *74*(12), 1686–1689.

Shao, H., Huang, M., Fu, H., Wang, S., Wang, L., Lu, J., Wang, Y., & Yu, K. (2019). Hollow WO3/SnO2 hetero-nanofibers: controlled synthesis and high efficiency of acetone vapor detection. *Frontiers in Chemistry*, *7*, 785.

Sharma, J., Vashishtha, M., & Shah, D. O. (2014). Crystallite size dependence on structural parameters and photocatalytic activity of microemulsion mediated synthesized ZnO nanoparticles annealed at different temperatures. *Global Journal of Science Frontier Research*, *14*(5), 18–32.

Singh, G., Singh, A., Singh, P., Shukla, R., Tripathi, S., & Mishra, V. K. (2021). The Fate of Organic Pollutants and Their Microbial Degradation in Water Bodies. *Pollutants and Water Management: Resources, Strategies and Scarcity*, 210–240.

Singh, P., Priya, B., Shandilya, P., Raizada, P., Singh, N., Pare, B., & Jonnalagadda, S. B. (2019). Photocatalytic mineralization of antibiotics using 60% WO3/BiOCl stacked to graphene sand composite and chitosan. *Arabian Journal of Chemistry*, *12*(8), 4627–4645.

Stojadinović, S., Vasilić, R., Radić, N., Tadić, N., Stefanov, P., & Grbić, B. (2016). The formation of tungsten doped Al2O3/ZnO coatings on aluminum by plasma electrolytic oxidation and their application in photocatalysis. *Applied Surface Science*, *377*, 37–43.

Sun, J., Li, X., Quan, Y., Yin, Y., & Zheng, S. (2015). Effect of long-term organic removal on ion exchange properties and performance during sewage tertiary treatment by conventional anion exchange resins. *Chemosphere*, *136*, 181–189.

Sun, M., Kong, W., Zhao, Y., Liu, X., Xuan, J., Liu, Y., Jia, F., Yin, G., Wang, J., & Zhang, J. (2019). Improving photocatalytic degradation activity of organic pollutant by Sn4+ doping of anatase TiO2 hierarchical nanospheres with dominant {001} facets. *Nanomaterials*, *9*(11), 1603.

Szilagyi, I. M., Madarász, J., Pokol, G., Király, P., Tárkányi, G., Saukko, S., Mizsei, J., Toth, A. L., Szabó, A., & Varga-Josepovits, K. (2008). Stability and controlled composition of hexagonal WO3. *Chemistry of Materials*, *20*(12), 4116–4125.

Theiss, W. (2002). Analysis of optical spectra by computer simulation-from basics to batch mode. *Theiss Hard-Und Software for Optical Spectroscopy: Aachen, Germany*. *Retrieved From*.

Thiagarajan, S., Sanmugam, A., & Vikraman, D. (2017). Facile methodology of sol-gel synthesis for metal oxide nanostructures. *Recent Applications in Sol-Gel Synthesis*, 1–17.

Trochowski, M., Kobielusz, M., Mroz, K., Surówka, M., Hämäläinen, J., Iivonen, T., Leskelä, M., & Macyk, W. (2019). How insignificant modifications of photocatalysts can significantly change their photocatalytic activity. *Journal of Materials Chemistry A*, *7*(43), 25142–25154.

Tseng, T. K., Lin, Y. S., Chen, Y. J., & Chu, H. (2010). A review of photocatalysts prepared by sol-gel method for VOCs removal. *International Journal of Molecular Sciences*, *11*(6), 2336–2361.

Ubi, G. M., Ikpeme, E. V, & Essien, I. S. (2022). Essentials of the COVID-19 coronavirus. In *Data Science for COVID-19* (pp. 1–25). Elsevier.

United Nation. (2022). *Water and Sanitation*. United Nations Sustainable Development. https://www.un.org/sustainabledevelopment/water-and sanitation

Vamvasakis, I., Georgaki, I., Vernardou, D., Kenanakis, G., & Katsarakis, N. (2015). Synthesis of WO 3 catalytic powders: Evaluation of photocatalytic activity under NUV/visible light irradiation and alkaline reaction pH. *Journal of Sol-Gel Science and Technology*, *76*, 120–128.

Varghese, A. R., Amarendra, G., & Hussain, S. (2018). Cr: SnO2 thin films-synthesis and characterization. *AIP Conference Proceedings*, *1951*(1), 20017.

Wang, C., Wu, D., Wang, P., Ao, Y., Hou, J., & Qian, J. (2015). Effect of oxygen vacancy on enhanced photocatalytic activity of reduced ZnO nanorod arrays. *Applied Surface Science*, *325*, 112–116.

Wang, Y., Sun, C., Zhao, X., Cui, B., Zeng, Z., Wang, A., Liu, G., & Cui, H. (2016). The application of nano-TiO 2 photo semiconductors in agriculture. *Nanoscale Research Letters*, *11*, 1–7.

World Heath Organization. (2022). *Drinking-water*. World Health Organization. https://www.who.int/news-room/fact-sheets/detail/drinking-water

Yadav, B. C., Dixit, R., & Singh, S. (2014). A review on synthesis, fabrication, and properties of nanostructured pure and doped tin oxide films. *International Journal of Scientific and Innovative Research*, *2*(1), 41–57.

Yang, L., Wang, F., Shu, C., Liu, P., Zhang, W., & Hu, S. (2016). An in-situ synthesis of Ag/AgCl/TiO2/hierarchical porous magnesian material and its photocatalytic performance. *Scientific Reports*, *6*(1), 21617.

Yimsiri, P., & Mackley, M. R. (2006). Spin and dip coating of light-emitting polymer solutions: Matching experiment with modelling. *Chemical Engineering Science*, *61*(11), 3496–3505.

Yıldırım, M. A., Akaltun, Y., & Ateş, A. (2012). Characteristics of SnO2 thin films prepared by SILAR. *Solid State Sciences*, *14*(9), 1282–1288.

Yousefi, S. R., Alshamsi, H. A., Amiri, O., & Salavati-Niasari, M. (2021). Synthesis, characterization and application of Co/Co3O4 nanocomposites as an effective photocatalyst for discoloration of organic dye contaminants in wastewater and antibacterial properties. *Journal of Molecular Liquids*, *337*, 116405.

Yousefi, S. R., Amiri, O., & Salavati-Niasari, M. (2019). Control sonochemical parameter to prepare pure Zn0. 35Fe2. 65O4 nanostructures and study their photocatalytic activity. *Ultrasonics Sonochemistry*, *58*, 104619.

Yousefi, S. R., Ghanbari, D., Salavati-Niasari, M., & Hassanpour, M. (2016). Photo-degradation of organic dyes: simple chemical synthesis of Ni (OH) 2 nanoparticles, Ni/Ni (OH) 2 and Ni/NiO magnetic nanocomposites. *Journal of Materials Science: Materials in Electronics*, *27*, 1244–1253.

Yousefi, S. R., Ghanbari, M., Amiri, O., Marzhoseyni, Z., Mehdizadeh, P., Hajizadeh- Oghaz, M., & Salavati- Niasari, M. (2021). Dy2BaCuO5/Ba4DyCu3O9. 09 S- scheme heterojunction nanocomposite with enhanced photocatalytic and antibacterial activities. *Journal of the American Ceramic Society*, *104*(7), 2952–2965.

Yousefi, S. R., Sobhani, A., Alshamsi, H. A., & Salavati-Niasari, M. (2021). Green sonochemical synthesis of BaDy 2 NiO 5/Dy 2 O 3 and BaDy 2 NiO 5/NiO nanocomposites in the presence of core almond as a capping agent and their application as photocatalysts for the removal of organic dyes in water. *RSC Advances*, *11*(19), 11500–11512.

Yousefi, S. R., Sobhani, A., & Salavati-Niasari, M. (2017). A new nanocomposite superionic system (CdHgI4/HgI2): synthesis, characterization and experimental investigation. *Advanced Powder Technology*, *28*(4), 1258–1262.

Zarei, S., Hasheminiasari, M., Masoudpanah, S. M., & Javadpour, J. (2022). Photocatalytic properties of ZnO/SnO2 nanocomposite films: role of morphology. *Journal of Materials Research and Technology*, *17*, 2305–2312.

Zhang, L., Wang, W., Zhou, L., & Xu, H. (2007). Bi2WO6 nano- and microstructures: shape control and associated visible- light- driven photocatalytic activities. *Small*, *3*(9), 1618–1625.

Zhu, D., & Zhou, Q. (2019). Action and mechanism of semiconductor photocatalysis on degradation of organic pollutants in water treatment: A review. *Environmental Nanotechnology, Monitoring & Management*, *12*, 100255.

APPENDICES

Appendix 1: Introduction Letter from the Institution

KABARAK UNIVERSITY
OFFICE OF THE DIRECTOR
INSTITUTE OF POST GRADUATE STUDIES

Private Bag - 20157
KABARAK, KENYA
E-mail: directorpostgraduate@kabarak.ac.ke
http://kabarak.ac.ke/institute-postgraduate-studies/

20th June 2023

The General
National Commission for Science, Technology & Innovation (NACOSTI)
P.O. Box 30623 – 00100
NAIROBI

Dear Sir/Madam,

RE: VICTOR ISAHI – GMP/M/0693/05/21

The above named is a student at Kabarak University. He is carrying out a research entitled **"Investigation of Photocatalytic Effect of WO_3/SnO_2 Thin Films for Contaminated Water Treatment"**

The student has been granted approval for ethical clearance by Kabarak University Research Ethics Committee and is ready to undertake field research.

Kindly provide the student with a research permit to enable him to undertake the research.

Thank you.

KABARAK UNIVERSITY
DIRECTOR
POST GRADUATE STUDIES
20 JUN 2023
PRIVATE BAG - 20157, KABARAK

Dr. Nehemiah Kiplagat, PhD
Ag. Director, Institute of Postgraduate Studies

Kabarak University Moral Code
As members of Kabarak University family, we purpose at all times and in all places, to set apart in one's heart, Jesus as Lord.
(1 Peter 3:15)

Kabarak University is ISO 9001:2015 Certified

Appendix II: KUREC Clearance Letter

KABARAK UNIVERSITY RESEARCH ETHICS COMMITTEE

Private Bag - 20157
KABARAK, KENYA
Email: kurec@kabarak.ac.ke

Tel: 254-51-343234/5
Fax: 254-051-343529
www.kabarak.ac.ke

OUR REF: KABU01/KUREC/001/06/06/23 **Date: 13th June, 2023**

Victor Isahi,
Reg. No: GMP/M/0693/05/21
Kabarak University,

Dear Victor,

RE: INVESTIGATION OF PHOTOCATALYTIC EFFECT OF *WO3/SnO2* THIN FILMS FOR CONTAMINATED WATER TREATMENT

This is to inform you that ***KUREC*** has reviewed and approved your above research proposal. Your application approval number is ***KUREC-060623.*** The approval period is ***13/06/2023 – 13/06/ 2024.***

This approval is subject to compliance with the following requirements:

i. All researchers shall obtain an introduction letter to NACOSTI from the relevant head of institutions (Institute of postgraduate, School dean or Directorate of research)
ii. The researcher shall further obtain a RESEARCH PERMIT from NACOSTI before commencement of data collection & submit a copy of the permit to **KUREC.**
iii. Only approved documents including (informed consents, study instruments, MTA Material Transfer Agreement) will be used
iv. All changes including (amendments, deviations, and violations) are submitted for review and approval by ***KUREC***:
v. Death and life-threatening problems and serious adverse events or unexpected adverse events whether related or unrelated to the study must be reported to ***KUREC*** within 72 hours of notification;
vi. Any changes, anticipated or otherwise that may increase the risk(s) or affected safety or welfare of study participants and others or affect the integrity of the research must be reported to ***KUREC*** within 72 hours;
vii. Clearance for export of biological specimens must be obtained from relevant institutions and submit a copy of the permit to KUREC;
viii. Submission of a request for renewal of approval at least 60 days prior to expiry of the approval period. Attach a comprehensive progress report to support the renewal and;
ix. Submission of an executive summary report within 90 days upon completion of the study to ***KUREC***

Sincerely,

KABARAK UNIVERSITY
INSTITUTIONAL RESEARCH ETHICS COMMITTEE
15 SEP 2023
APPROVED

Prof. Jackson Kitetu PhD.
KUREC-Chairman

Cc Vice Chancellor
DVC-Academic & Research
Registrar-Academic & Research
Director-Research Innovation & Outreach
Institute of Post Graduate Studies

Appendix III: NACOSTI Permit Research

REPUBLIC OF KENYA

NATIONAL COMMISSION FOR SCIENCE,TECHNOLOGY & INNOVATION

Ref No: **695914**

Date of Issue: **30/June/2023**

RESEARCH LICENSE

This is to Certify that Mr.. Victor Isahi of Kabarak University, has been licensed to conduct research as per the provision of the Science, Technology and Innovation Act, 2013 (Rev.2014) in Nakuru on the topic: INVESTIGATION OF PHOTOCATALYTIC EFFECT OF WO3/SnO2 THIN FILMS FOR CONTAMINATED WATER TREATMENT for the period ending : 30/June/2024.

License No: **NACOSTI/P/23/27489**

695914

Applicant Identification Number

Director General
NATIONAL COMMISSION FOR SCIENCE,TECHNOLOGY & INNOVATION

Verification QR Code

NOTE: This is a computer generated License. To verify the authenticity of this document, Scan the QR Code using QR scanner application.

See overleaf for conditions

Appendix IV: List of Publication

Tanzania Journal of Science 49(3): 629-641, 2023
ISSN 0856-1761, e-ISSN 2507-7961

Optical Characterization of Photocatalytic Tungsten Oxide/Tin Oxide (WO_3/SnO_2) Thin Films for Use in Degradation of Water Pollutants

Victor Isahi[1*], Christopher Maghanga[1], Mghendi Mwamburi[2], Onesmus Munyati[3], Sylvester Hatwaambo[4], Emmanuel Akoto[1], Wycliffe Isoe[5] and Mir Waqas Alam[6]

[1]*Department of Biological & Physical Sciences, Kabarak University, P.O. Box Private Bag, 20157, Kabarak, Kenya.*

[2]*Department of Physics, University of Eldoret, P.O. Box 1125 - 30100, Eldoret, Kenya.*

[3]*Departmet of Chemistry, University of Zambia, P.O. Box 32379, Lusaka, Zambia.*

[4]*Department of Physics, University of Zambia, P.O. Box 32379, Lusaka, Zambia.*

[5]*Department of Physics, Masinde Muliro University, P.O. Box 190 -50100, Kakamega, Kenya.*

[6]*Department of Physics, College of Science, King Faisal University, P.O. Box 400, Al-Ahsa 31982, Saudi Arabia.*

**Corresponding author, email: visahi@kabarak.ac.ke*

Received 20 Jul 2023, Revised 11 Sep 2023, Accepted 15 Sep 2023 Published Sep 2023

DOI: https://dx.doi.org/10.4314/tjs.v49i3.7

Abstract

Organic pollutants in water have been a challenge and pose significant risks to human health. As a result, research efforts to eliminate these pollutants have been on the rise. Photocatalysis has shown incredible potential in water treatment containing organic pollutants since it is affordable and utilizes solar energy. Tin oxide (SnO_2) has ardently been investigated as a photocatalyst for water treatment due to its remarkable properties such as; non-toxicity, and stability. However, its wide band gap and the tendency for some electrons and holes to recombine during its use have been cited to be among limiting factors affecting its effectiveness. This study, therefore, aimed to optimize SnO_2 thin films by doping it with varied proportions of Tungsten oxide (WO_3) using Sol-gel technique and investigating the effects of WO_3 doping on the optical and photocatalytic properties of the prepared films. From the results, the calculated rate constants for SnO_2 and WO_3/SnO_2(1.5%wt.) were 0.00256 min^{-1} and 0.00519 min^{-1}, respectively, and the corresponding band gaps were 3.82 and 3.03 eV, suggesting that doping improved the optical absorbance of the films and caused a red shift of the absorption edge of the films. These results show WO_3/SnO_2 is a good candidate for photocatalytic water treatment.

Keywords: Doping, sol-gel, photocatalysis, optical characterization, WO_3/SnO_2

Introduction

Globally, one in three individuals living today do not have adequate access to safe drinking water (United Nations 2022). A World Health Organization (WHO) report indicates that contaminated drinking water can transmit diseases such as diarrhea, cholera, dysentery, typhoid, and polio, which cause many deaths annually (Buchholz 2022, World Heath Organization 2022). Organic substances are one of the major pollutants in contaminated water that are as a result of substances such as toxic dye effluents discharged from various industries which contaminate rivers and other water resources (Manikandan et al. 2018, Ojha and Tiwary 2021). Therefore, research related to finding affordable, effective, and healthy approaches to eliminate these toxic dyes has been on the rise in recent years. Among various

Appendix V: Evidence of Conference Participation

MSSEESA

2022 MSSEESA Material Science Conference 16th-18th November 2022

THIS IS TO CERTIFY THAT

Victor Isahi

PRESENTED A PAPER TITLED : *INFLUENCE OF POST ANNEALING TEMPERATURE ON TIN (IV) OXIDE FILMS PREPARED BY SOL-GEL SPIN COATING TECHNIQUE FOR IMPROVEMENT OF OPTICAL PROPERTIES*

ON 17TH NOVEMBER 2022

HELD AT ROYAL GARDENS HOTEL, NAKURU, KENYA

CHIEF COORDINATOR, MSSEESA

Appendix VI: Research Acknowledgment from the University of Zambia

UNIVERSITY OF ZAMBIA
School of Natural Sciences
Department of Physics

P.O. Box 32379
Lusaka 10101, ZAMBIA
Email: shatwaambo@unza.zm

Tel: +260-211-290429
Tel/Fax: +260-211-293343
Mobile: +260 977 117 931

2nd March 2023

Victor Isahi (Mr.)
Kabarak University
Department of Biology and Physical Sciences
Private Bag 20157
Kabarak,
KENYA

RESEARCH FELLOWSHIP VICTOR ISAHI

This is to acknowledge that Mr. Victor Isahi is a Masters student in Physics at the Kabarak University, in Kenya and that he has conducted his research on Material Science at the University of Zambia, School of Natural Sciences, in the Departments of Chemistry and Physics for six (6) months, as part of the student exchange program funded by the International Science Programme (ISP) of Uppsala University in Sweden through the Material Science and Solar Energy Network for Eastern and Southern Africa (MSSESSA).

During his research visit, he was able to synthesize and prepare materials using various techniques, as well as learning how to characterize materials using techniques such as UV-Vis Spectroscopy, Atomic Force Microscopy, I-V Four Point Probe Measurements, Cyclic Voltammetry, and X-Ray Diffraction technique (XRD). His overall research activities were impressive. We wish, Mr. Isahi a very successful completion of Master of Science in Physics programme at the Kabarak University.

Thank you,

Dr. Sylvester Hatwaambo
Coordinator – MSSEESA, Zambia Chapter